IL-32 Promotes Angiogenesis

Claudia A. Nold-Petry, Ina Rudloff, Yvonne Baumer, Menotti Ruvo, Daniela Marasco, Paolo Botti, Laszlo Farkas, Steven X. Cho, Jarod A. Zepp, Tania Azam, Hannah Dinkel, Brent E. Palmer, William A. Boisvert, Carlyne D. Cool, Laima Taraseviciene-Stewart, Bas Heinhuis, Leo A. B. Joosten, Charles A. Dinarello, Norbert F. Voelkel and Marcel F. Nold

J Immunol 2014; 192:589-602; Prepublished online 11 December 2013;
doi: 10.4049/jimmunol.1202802
http://www.jimmunol.org/content/192/2/589

The Journal of Immunology is published twice each month by
The American Association of Immunologists, Inc.,
9650 Rockville Pike, Bethesda, MD 20814-3994.

Print ISSN: 0022-1767 Online ISSN: 1550-6606.

IL-32 Promotes Angiogenesis

Claudia A. Nold-Petry,* Ina Rudloff,* Yvonne Baumer,† Menotti Ruvo,‡ Daniela Marasco,§ Paolo Botti,¶ Laszlo Farkas,‖ Steven X. Cho,* Jarod A. Zepp,# Tania Azam,# Hannah Dinkel,# Brent E. Palmer,# William A. Boisvert,† Carlyne D. Cool, Laima Taraseviciene-Stewart,# Bas Heinhuis,†† Leo A. B. Joosten,†† Charles A. Dinarello,#,†† Norbert F. Voelkel,**,[1] and Marcel F. Nold*,[1]**

IL-32 is a multifaceted cytokine with a role in infections, autoimmune diseases, and cancer, and it exerts diverse functions, including aggravation of inflammation and inhibition of virus propagation. We previously identified IL-32 as a critical regulator of endothelial cell (EC) functions, and we now reveal that IL-32 also possesses angiogenic properties. The hyperproliferative ECs of human pulmonary arterial hypertension and glioblastoma multiforme exhibited a markedly increased abundance of IL-32, and, significantly, the cytokine colocalized with integrin $\alpha_V\beta_3$. Vascular endothelial growth factor (VEGF) receptor blockade, which resulted in EC hyperproliferation, increased IL-32 three-fold. Small interfering RNA–mediated silencing of IL-32 negated the 58% proliferation of ECs that occurred within 24 h in scrambled-transfected controls. Reduction of IL-32 neither affected apoptosis (insignificant changes in Bak-1, Bcl-2, Bcl-x_L, lactate dehydrogenase, annexin V, and propidium iodide) nor VEGF or TGF-β levels, but siIL-32–transfected adult and neonatal ECs produced up to 61% less NO, IL-8, and matrix metalloproteinase-9, and up to 3-fold more activin A and endostatin. In coculture-based angiogenesis assays, IL-32γ dose-dependently increased tube formation up to 3-fold; an $\alpha_V\beta_3$ inhibitor prevented this activity and reduced IL-32γ–induced IL-8 by 85%. In matrigel plugs loaded with IL-32γ, VEGF, or vehicle and injected into live mice, we observed the anticipated VEGF-induced increase in neocapillarization (8-fold versus vehicle), but unexpectedly, IL-32γ was equally angiogenic. A second signal such as IFN-γ was required to render cells responsive to exogenous IL-32γ; importantly, this was confirmed using a completely synthetic preparation of IL-32γ. In summary, we add angiogenic properties that are mediated by integrin $\alpha_V\beta_3$ but VEGF-independent to the portfolio of IL-32, implicating a role for this versatile cytokine in pulmonary arterial hypertension and neoplastic diseases. ***The Journal of Immunology*****, 2014, 192: 589–602.**

Since its designation as a cytokine by Kim and colleagues in 2005 (1), considerable progress has been made with elucidating the properties of the unusual cytokine IL-32. Structurally, IL-32 does not share similarities with known cytokine families (1). Seven isoforms, IL-32α–ζ (1, 2), and one additional isoform (3) have been described and alternative splicing appears to have biological relevance. For example, in endothelial cells (ECs), an isoform switch from α/γ to β/ε occurs upon stimulation with IL-1β or thrombin (4), and a protective function for this splicing event has been suggested (5). Moreover, an isoform switch from IL-32γ to IL-32β in tissues from patients with rheumatoid arthritis is associated with an attenuation of inflammation (6). A receptor for IL-32 is currently unknown, although ligand-affinity column assays have shown that IL-32 can bind to neutrophil proteinase-3 (7), and that subsequent processing alters the biological activity of IL-32α and IL-32γ (8).

The earlier studies on IL-32 focused mainly on its proinflammatory properties, for example the induction of other cytokines and chemokines such as IL-1β, IL-6, and TNF, as well as Th1 and Th17-associated cytokines, in various cells via activation of the p38 MAPK, NF-κB, and AP-1 signal transduction pathways (1, 9). IL-32 is present in increased abundance in a variety of diseases, including chronic obstructive pulmonary disease (10), inflammatory bowel disease and psoriasis (11), allergic rhinitis (12), and myasthenia gravis (13), and its levels are directly related to disease severity in rheumatoid arthritis (14, 15).

We and others have shown that IL-32 possesses antiviral properties. For instance, silencing of IL-32 by small interfering (si) RNA (siIL-32) resulted in increased production of HIV-1 (9) as well as higher viral loads of vesicular stomatitis virus and HSV-2 (16). In each of these models, the abundance of IFNs was dependent on the levels of IL-32, but the antiviral activity of IL-32 was only in part via type I IFNs. IL-32 has also been implicated in

*Ritchie Centre, Monash Institute of Medical Research, Monash University, Melbourne, Victoria 3168, Australia; †Center for Cardiovascular Research, John A. Burns School of Medicine, University of Hawaii, Honolulu, HI 96813; ‡Istituto di Biostrutture e Bioimmagini, Consiglio Nazionale delle Ricerce e Centro Interuniversitario di Ricerca sui Peptidi Bioattivi, 80134 Naples, Italy; §Department of Pharmacy, University of Naples Federico II, 80134 Naples, Italy; ¶ArisGen SA, 1228 Plan-les-Ouates, Switzerland; ‖Department of Internal Medicine, Virginia Commonwealth University, Richmond, VA 23298; #Department of Medicine, University of Colorado Denver, Aurora, CO 80045; **Department of Pathology, University of Colorado Denver, Aurora, CO 80045; and ††Radboud University Medical Center, 6500 HB Nijmegen, The Netherlands

[1]N.F.V. and M.F.N. contributed equally to this work.

Received for publication October 5, 2012. Accepted for publication September 5, 2013.

This work was supported by Deutsche Forschungsgemeinschaft Grant 747/1-1 (to M.F.N.), National Institutes of Health Grants AI-15614 and CA-04 6934 (to C.A.D.), and by the Victorian Government (Australia) Operational Infrastructure Support Program.

Address correspondence and reprint requests to Prof. Norbert F. Voelkel at the current address: Pulmonary and Critical Care Medicine Division, Molecular Medicine Research Building, Broad Street, Virginia Commonwealth University, Richmond, VA 23298, or Prof. Marcel F. Nold, Monash Institute of Medical Research, 27-31 Wright Street, Clayton, VIC 3168, Australia. E-mail addresses: nvoelkel@mcvh-vcu.edu (N.F.V.) or mfnold@hotmail.com (M.F.N.)

Abbreviations used in this article: EC, endothelial cell; GBM, glioblastoma multiforme; HAoEC, human aortic endothelial cell; HSF, human skin fibroblast; MMP, matrix metalloproteinase; PAH, pulmonary arterial hypertension; PI, propidium iodide; PMN, polymorphonuclear cell; siIL-32, small interfering RNA to IL-32; siRNA, small interfering RNA; VEGF, vascular endothelial growth factor; vWF, von Willebrand factor.

the immune response to influenza A (17), hepatitis B (18) and C (19), papillomavirus (20), and the Venezuelan equine encephalitis virus (21).

With regard to neoplastic diseases, IL-32 has been demonstrated to modulate apoptosis in myelodysplastic syndromes and chronic myeloid leukemia (22). IL-32 also exhibited antiapoptotic properties in pancreatic cancer cells (23) and was associated with a more malignant phenotype in tumors of the lung (24). Conversely, IL-32γ overexpression by transgene or cell transfer inhibited the growth of melanomas and colon tumors (25).

In ECs of various origin, IL-32 is a crucial mediator of proinflammatory stimuli such as IL-1β, thrombin, LPS, and platelets. We found that the abundance of IL-32 was increased by treatment with these triggers of EC inflammation, and silencing by siIL-32 resulted in decreased production of proinflammatory IL-1α, IL-6, IL-8, and ICAM-1, as well as increased expression of thrombomodulin/CD141 (4). Furthermore, IL-32 has been shown to mediate giant cell arteritis (26), to interact with integrins (27), and to play an important role at multiple levels in atherosclerosis (5).

A dysregulation of the functions of ECs plays a major role in pulmonary arterial hypertension (PAH). Several forms of PAH have been classified, but many of them are characterized by complex pulmonary vascular lesions. These lesions are multicellular and demonstrate hyperproliferative ECs that grow in an uncontrolled fashion to the point of obliteration of the vascular lumen (28). Mechanisms likely involved in this pulmonary microvessel disease have recently been reviewed (29, 30). Importantly, the proliferating ECs are apoptosis-resistant and form multiple lumina, often with the appearance of glomeruloid structures or structures that are reminiscent of the vascular coils observed in the tumors of glioblastoma multiforme (GBM), a tumor that originates from EC precursors (31). Increasingly a role for inflammatory cytokines and immune cells in PAH is being recognized (32, 33); for example, IL-1 and IL-6 plasma levels are increased in patients with severe PAH (32). Although a consensus is building that inflammation and immune mechanisms play a role in the pathobiology of severe forms of PAH, little is known as to whether inflammation causes the formation of the vascular lesions or how inflammatory cells and immune cells contribute to the angio-obliteration (angiogenesis) of these remodeled lung vessels (34).

Because IL-32 acts as an important regulator of EC biology (4), and because the prototypical angiogenic mediator vascular endothelial growth factor (VEGF) is highly expressed in plexiform vascular lung lesions (35), as well as in psoriatic angioproliferative skin lesions (36), we asked whether IL-32 could also function as an angiogenic factor.

Materials and Methods

Reagents

HUVECs media and additives were from Lonza (Walkersville, MD) or from PromoCell (Heidelberg, Germany; ECGM MV, used in the coculture experiments). Iscove's DMEM, RPMI 1640, and M199 were obtained from Life Technologies/Invitrogen (Carlsbad, CA). Human skin fibroblasts (HSFs) and their medium (FGM2) were from PromoCell. PBS, FCS, and penicillin/streptomycin were purchased from Cellgro (Herndon, VA). Pooled human serum and Accutase were acquired from MP Biomedicals (Solon, OH). LPS (O55:B5) was from Sigma-Aldrich (St. Louis, MO). The Nucleofector II electroporation device and reagents as well as primocin were from Amaxa (Cologne, Germany). siIL-32 was purchased from Thermo Fisher Scientific (Lafayette, CO) and comprised four ON-TARGETplus duplexes (I–IV) with the antisense sequences I, 5′-UAA UAA GCC GCC ACU GUC UUU-3′; II, 5′-CCG UAA UCC AUC UCU UUC UUU-3′; III, 5′-UCA UCA GAG AGG ACC UUC GUU-3′; and IV, 5′-CAA GUA GAG GAG UGA GCU CUU-3′. One sequence comprised a quarter of the total siRNA concentration; that is, 25 nM of each sequence was pooled for a total siRNA concentration of 100 nM used in the transfections. Scrambled siRNA (silencer negative control no. 1) was purchased from Ambion (Austin, TX). Recombinant human IL-32γ and IL-1β and recombinant murine VEGF were from R&D Systems (Minneapolis, MN). As per the manufacturer, the endotoxin level in recombinant human IL-32γ was <1 endotoxin unit per microgram by the *Limulus* amebocyte lysate method. All other recombinant cytokines were bought from PeproTech (Rocky Hill, NJ). We generated the affinity-purified anti-human IL-32 Ab and have used it previously (1, 9). FITC-labeled *Sambucus nigra* lectin was from Vector Laboratories (Burlingame, CA). The $\alpha_V\beta_3$ inhibitor cyclo(Arg-Gly-Asp-D-Phe-Val) was obtained from Enzo Life Sciences (Farmingdale, NY).

Generation of synthetic IL-32γ

The chemical synthesis of IL-32γ (103 residues) was performed following a four-fragment strategy of native chemical ligation. Fragments used to assemble the protein were 1) the N-terminal fragment, residues 1–35-Cα-COS-R (F1); 2) the intermediate fragment, residues 36–56-Cα-COS-R with an N-terminal Cys introduced as thiazolidine (F2a); 3) another intermediate fragment, residues 57–59-Cα-COS-R with an N-terminal Cys introduced as thiazolidine (F2b); and 4) the C-terminal fragment, residues 60–103 (F3). F1, F2a, and F2b were assembled by the solid phase method on a β-mercapto-propionic acid-glycine resin to generate C-terminal thioesters with R indicating β-mercapto-propionic acid-glycine, following Boc protocols with in situ neutralization and using related chemicals (37). F3 was assembled by standard Fmoc chemistry on a Wang resin to afford a C-terminal–free polypeptide. After cleavage, polypeptides were purified to homogeneity by reversed phase HPLC and characterized by liquid chromatography/mass spectrometry to assess purity and identity. Native chemical ligation and thiazolidine opening reactions were performed as reported elsewhere (37). The intermediate ligated polypeptides IL-32 (57–103), IL-32 (36–103), and the final full-length 103 residue products were also purified by reversed phase HPLC and characterized by liquid chromatography/mass spectrometry to assess purity and identity: F1, expected M_r of 4,011.6 kDa, found 4,011.4 (purity 90%); F2a, expected M_r of 2,760.4 kDa, found 2,760.0 (purity 95%); F2b, expected M_r of 560.1 kDa, found 560.0 (purity 97%); F3, expected M_r of 5,042.5, found 5,043.0 (purity 95%); full-length IL-32γ, expected M_r of 11,570.4 kDa, found 11,570.3 (purity >95%). The single-letter code sequence of the full-length IL-32γ is as follows, with the ligation sites in bold and underlined: MCFPKVLSDD MKKLKARMVM LLPTSAQGLG AWVS**AC**DTKD TVGHPGPWRD KDPAL**WC**Q**LC** LSSQHQAIER FYDKMQNAES GRGQVMSSLA ELEDDFKEGY LET.

Cell culture

HUVECs were isolated from human umbilical cords after informed consent was obtained from the parents. All experiments were approved by the Colorado Multiple Institutional Review Board. Cords were cleaned by several high-volume rinses with HBSS. Thereafter, one end of the cord was clamped and a catheter was inserted from the open end, through which the umbilical vein was filled with 0.3% trypsin (Life Technologies). The catheter was removed and the open end was clamped before the cord was incubated for 30 min at 37°C. Thereafter, the cord was massaged, the clamp was removed, and the cord was squeezed lengthwise to force the content into a collection tube. Two washes with HBSS were used to detach residual cells from the vein. The collection tube was centrifuged at 300 × *g* for 10 min, the pellet was resuspended in HUVEC growth medium (39% Iscove's DMEM, 38.6% RPMI 1640, 20% FCS, 0.4% endothelial mitogen [Biomedical Technologies], 17.6 U/ml heparin, 1% penicillin/streptomycin) and transferred into cell culture flasks coated with 1% gelatin. For stimulation, the medium was changed to endothelial cell stimulation medium comprising M199 (Life Technologies) with 2% FCS, 10 ng/ml human acidic fibroblast growth factor (PeproTech), 1% penicillin/streptomycin, and 17.6 U/ml heparin.

Aortic macrovascular ECs as well as coronary and pulmonary microvascular ECs were obtained from Lonza. Coronary and pulmonary ECs were cultured in EGM-2-MV (Lonza) with a final concentration of 5% FCS. Aortic ECs were grown in EGM-2 with a final concentration of 2% FCS.

PBMCs were isolated and cultured as described previously (38).

For the coculture experiments, HSFs were cultivated in a 48-well plate (5×10^4 cells/well) and grown to confluence for 3 d in FGM2 plus Supplement Mix (PromoCell). At day 3, HUVECs (5×10^4 cells/well) were carefully added to the confluent HSFs. After 4 h of incubation, HUVECs were attached and the incubation media were exchanged with a 1:1 mixture of ECGM MV and FGM2 (plus the respective supplement mix) with or without IL-32 (10, 25, 100 ng/ml) and with or without cyclo (Arg-Gly-Asp-D-Phe-Val) (10 μM). Treatment with recombinant human VEGF-165 (40 ng/ml) was used as internal assay control. The cells were

cocultured for 7 d with two media changes at 37°C and 5% CO_2. Both HUVECs and HSFs were used in passages two through eight and passaged using a DetachKit (PromoCell).

Transfections

HUVECs were detached, counted, centrifuged at 200 × *g* for 12 min, and subjected to electroporation using the Amaxa HUVEC Nucleofector kit and program U001. One cuvette contained 0.8×10^6 cells in 100 μl Nucleofector solution and 25–333 nM either siIL-32 or scrambled. Immediately after electroporation, the cells were incubated in 300 μl prewarmed M199 for 5 min. Thereafter, 0.2×10^6 cells were transferred into gelatinized six-well plates (Greiner Bio-One, Ocala, FL) to a final volume of 1 ml growth medium and allowed to recover overnight. On the next day, the medium was replaced with stimulation medium and the cells were stimulated.

Immunohistochemistry

Briefly, after paraffin-embedded sections were cut at 5-μm sections, the slides were deparaffinized and transferred through progressive ethanol gradients for rehydration. High-temperature Ag retrieval was performed in 10 mM/l citrate buffer (pH 6.0) for 30 min. Endogenous peroxidase was quenched with 3% hydrogen peroxide for 15 min twice. All immunostains were performed using the Dako Universal LSAB+ kit/HRP-based visualization kit. Primary Ab incubation was performed at 1:1500 dilution for 30 min. Chromagen development was performed with 3,3′-diaminobenzidine and counterstained with hematoxylin. Normal blocking serum without primary Ab was used for the negative control.

Immunofluorescence and confocal microscopy

Paraffin-embedded human lung tissue, obtained from patients with idiopathic PAH, and control tissue from patients without pulmonary vascular disease were used for double immunofluorescence. First, slides were steamed for 20 min in 0.01 M citrate buffer (pH 6.0) and blocked with 1% normal swine serum for 15 min. Primary Ab no. 1, IL-32 (1:50; Abcam, Cambridge, MA), was applied overnight at 4°C in 1% normal swine serum. Secondary Ab no. 1, anti-rabbit Alexa Fluor 594 (1:100; Invitrogen, Carlsbad, CA), was incubated for 4 h at room temperature in PBS. Sections were incubated with primary Ab no. 2, anti-mouse von Willebrand factor (vWF) (1:20; LifeSpan Biosciences, Seattle, WA), overnight at 4°C in PBS, then secondary Ab no. 2, anti-mouse Alexa Fluor 488 (1:100; Invitrogen), was applied for 4 h at room temperature in PBS. Slides were counterstained with DAPI at 1:20,000 and mounted with SlowFade antifade (both from Invitrogen). Negative controls with unspecific IgG were run in parallel. Optical sections were acquired by laser- scanning confocal microscopy with a Leica TCS-SP2 confocal microscope and images were analyzed and arranged with ImageJ. Microscopy was performed at the Virginia Commonwealth University Department of Anatomy and Neurobiology Microscopy Facility.

Electrochemiluminescence assays and ELISAs

Human IL-6 and IL-32 were measured using specific Ab pairs and an Origen analyzer (Wellstat Diagnostics, Gaithersburg, MD) as described previously (9); Ab pairs for all cytokines were obtained from R&D Systems. The IL-6 ELISA was obtained from Elisakit.com (Scoresby, VIC, Australia). TGF-β1 was determined by ELISA (R&D Systems) according to the manufacturer's instructions. Recombinant cytokines for electrochemiluminescence or ELISA standards were obtained from R&D Systems or PeproTech.

Real-time PCR analysis

RNA was extracted from HUVECs using the RNA Mini kit (Bioline, Alexandria, NSW, Australia) and then quantified with the NanoDrop (ND-1000) spectrophotometer (Thermo Scientific, Wilmington, DE). RNA was reversely transcribed using a high-capacity cDNA reverse transcription kit (Applied Biosystems, Melbourne, VIC, Australia) as per the manufacturer's instructions. SYBR Green quantitative RT-PCRs were run on the Applied Biosystems 7900HT Fast RT-PCR system. Oligonucleotide primers (forward/reverse) were as follows: 18S, 5′-CCC CTC GAT GCT CTT AGC TG-3′ and 5′-CTT TCG CTC TGG TCC GTC TT-3′; activin A, 5′-GTT TGC CGA GTC AGG AAC AG-3′ and 5′-CCC TTT AAG CCC ACT TCC TC-3′; angiogenin, 5′-GCC GAG GAG CCT GTG TT-3′ and 5′-GCG CTT GTT GCC ATG AAT-3′; angiopoietin 2, 5′-AGC TAA GGA CCC CAC TGT TG-3′ and 5′-TGA AGG GTT ACC AAA TCC CAC T-3′; Bak-1, 5′-CCA CCA GCC TGT TTG AGA GT-3′ and 5′-AAA CTG GCC CAA CAG AAC CA-3′; Bcl-2, 5′-CGC GAC TCC TGA TTC ATT GG-3′ and 5′-CAG TCT ACT TCC TCT GTG ATG TTG T-3′; Bcl-x_L, 5′-ACT CTT CCG GGA TGG GGT AA-3′ and 5′-ACA AAA GTA TCC CAG CCG CC-3′; endoglin, 5′-GCC CCA CAA GTC TTG CAG AA-3′ and 5′-GCT TGG ATG CCT GGA GAG TC-3′; IL-8, 5′-ACT CCA AAC CTT TCC ACC CC-3′ and 5′-GCG GAA GAT GAC CTT CTC CT-3′; and u-plasminogen activator, 5′-GTC GTG AGC GAC TCC AAA GG-3′ and 5′-GAC TTA TCT ATT TCA CAG TGC TGC C-3′. No template controls were included in parallel for each gene master mix. The cycling conditions were as follows: denaturation at 95°C for 10 min, followed by 40 cycles of denaturation at 95°C for 15 s, annealing and elongation at 60°C for 1 min. These cycles were followed by a melt-curve analysis, 95°C for 15 s, 60°C for 15 s, followed by 95°C for 15 s. Relative expression quantification was calculated using Pffafl's method. All fold changes in gene expression were normalized to 18S mRNA.

MTS assay

The CellTiter cell proliferation assay was purchased from Promega (Madison, WI) and executed according to the manufacturer's instructions. Briefly, cells were transfected and 2000 cells in 100 μl stimulation medium were seeded into a 96-well plate. Cells were grown for 3 d, then 20 μl MTS reagent was added to each well, followed by a further 2 h incubation. Then the absorbance at 490 nm was recorded in a plate reader. The quantity of the formazan product as measured by the absorbance is proportional to the number of living cells in the cultures.

Determination of nitrate/nitrite

Supernatants from EC cultures were collected and assayed for total nitrate/nitrite concentration using a kit provided by Cayman Chemical (Ann Arbor, MI).

In vitro angiogenesis model

On day 7 of coculture, cells were washed with PBS, fixed with 2% paraformaldehyde (pH 7.4) for 10 min at room temperature, treated with 0.1% Triton X-100, and blocked with 2% BSA in PBS. Thereafter, the coculture was incubated with *Sambucus nigra* lectin-FITC (20 μg/ml) for 1 h at room termperature in the dark. Cell nuclei were labeled using DAPI. Cells were washed thoroughly, covered with PBS, and examined microscopically on an Axiovert (Carl Zeiss, Jena, Germany). Five fields of view per condition were randomly chosen and photographed. The number of visible branches was counted using ImageJ.

Matrigel-related procedures in vivo

All animal experiments were approved by the Colorado Multiple Institutional Review Board. Vehicle (NaCl 0.9%), VEGF, or rIL-32γ (both R&D Systems) was mixed with growth factor–reduced high-concentration matrigel (BD Biosciences, San Diego, CA) at 4°C. Thereafter, each mouse (male ICR mice) received an s.c. injection with two 200 μl aliquots of matrigel with nonidentical contents on the right and left sides of the abdominal wall. The mice were allowed free access to food and water for 14 d, followed by harvest of the plugs as described below.

Histopathological analysis and scoring of matrigel plugs

This analysis was performed by Premier Laboratory (Boulder, CO). Each of the scientists at Premier Laboratory was blinded to the content of the matrigel plugs. Matrigel plugs and the surrounding tissue, skin, and muscle were removed at necropsy and placed into 10% neutral buffered formalin. The plugs were bisected, processed, and embedded in paraffin. Multiple sections were cut, one was stained with H&E, and another was immunohistochemically stained for CD31 wherein slides were dewaxed in xylene and hydrated to water through a series of alcohol gradients. Prior to staining, the tissue sections were pretreated with a TRIS/EDTA (pH 9.0) target retrieval solution (Dako, K8004) and incubated for 2 h at 70°C. A 3.0% hydrogen peroxide solution was used for 5 min at room temperature to quench any endogenous peroxidase activity within the tissue. Serum-free protein block (Dako, X0909) was used to neutralize any charged molecules that may cause nonspecific Ab binding. The rat anti-mouse CD31/PECAM-1 Ab (Dianova, Hamburg, Germany) was applied to the tissue sections at a working concentration of 5.0 μg/ml (1:40) from the stock solution for 60 min at room temperature. The primary Ab was then conjugated with a biotinylated rabbit anti-rat Ig (Dako, E0468) at a concentration of 2.125 μg/ml (1:400) for 30 min at room temperature. The biotinylated secondary Ab was then amplified with a goat anti-rabbit–labeled polymer (Dako, K4003) for 30 min at room temperature. Thereafter, staining was developed with liquid diaminobenzidine for 5 min at room temperature (Dako, K3468). Counterstaining was developed with auto-

mated hematoxylin (Dako, S3301) for 10 min. The negative control solution for this immunohistochemical stain was an unconjugated rat IgG2a isotype Ab (AbD Serotec, MCA1124) that was used at the same working concentration as the primary Ab.

The H&E-stained slides were reviewed by a board-certified veterinary pathologist. The evaluation included the degree of fibrosis in the subcutis adjacent to each implant as well as the inflammatory response in the subcutis and the overall cellularity within each implant. For scoring the metrics identified in the figures, the most advanced changes within an implant were used for scoring. Neocapillaries were defined by the presence of oval-circular structures containing RBCs and associated with concentrically arranged mesenchymal nuclei (fibroblasts and endothelial cells). A subjective, semiquantitative scoring system was used: 0, no significant change; 1, minimal change; 2, mild change; 3, moderate change; and 4, marked change.

The CD31-stained slides were scanned on an Aperio ScanScope XT. Then the area of matrigel implant was traced and analyzed via Aperio's microvessel algorithm that calculated the number of vessels and microvessel density along with other parameters.

Statistical analysis

Datasets (raw data) were first tested for normality by the Kolmogorov–Smirnov method and equal variance (p value to reject 0.05) using the SigmaStat software (Systat Software, San Jose, CA). Thereafter, these data were analyzed by the appropriate statistical test, including Student t test, one-way ANOVA, and one-way ANOVA on ranks.

Results

IL-32 in tissue sections from patients with PAH and in an in vitro model of pulmonary angioproliferation induced by VEGF receptor blockade

We reported that IL-32 is important in EC biology (4). Therefore, a next reasonable step was to investigate the role of this cytokine in diseases that involve ECs. We stained tissue sections from patients with PAH using two different Abs against IL-32 (Fig. 1). In a normal human lung arteriole, IL-32 was detected in the vascular smooth muscle cells of the medial layer (shown in red in Fig. 1A), but not in the endothelial monolayer, as highlighted by vWF staining in green. On the other hand, the ECs in lung specimens from patients with idiopathic PAH did express IL-32. Fig. 1B shows a patent arteriole, with the arrowheads in the insets pointing to the IL-32$^+$ ECs. When we examined the characteristic plexiform lesions, which are diagnostic for idiopathic PAH (28, 31), we found a yet higher abundance of IL-32 within the hyperproliferative ECs that grow to obstruct the blood vessels. In the specimen in Fig. 1C, which was obtained from the same patient displayed in Fig. 1B, an arteriolar vessel is almost completely obliterated by the IL-32–expressing, hyperproliferative ECs. Some of these ECs, particularly in the center of the lesion, have very large nuclei (stained by DAPI in blue) and are activated, phenotypically switched cells that have lost the vWF marker. Fig. 1D and the insets show more detail at a higher magnification and the colocalization of vWF and IL-32 (arrows). Fig. 1E–H demonstrate a similar pattern of IL-32 expression when we used classical immunohistochemistry. The red arrowheads point to the expression of IL-32 in the proliferating ECs. We also found IL-32 in the bronchial epithelium (golden arrows), which was expected based on an earlier study (10). For negative control, we performed the staining in the absence of the primary Abs and observed no staining on any specimen (data not shown).

We previously reported that blockade of the VEGF receptor by the small molecule inhibitor semaxanib (Su5416) initially causes apoptosis. However, ECs surviving this initial phase become hyperproliferative and grow in an uncontrolled fashion, which can result in obstruction of the lumen of artificial capillaries (39), resembling the pathology of PAH (Fig. 1A–H). Hence, treatment of ECs with semaxanib can be regarded as a model of this disease, which we employed to confirm the immunohistochemistry results. As depicted in Fig. 1I, IL-32 protein levels increased up to 3.4-fold as HUVECs underwent the transformation into the hyperproliferative state. In three of four experiments, IL-32 expression peaked on day 3. However, in the ECs from the fourth cord, which, unlike the other HUVECs, contained considerably less IL-32 in semaxanib-treated cells than did vehicle-treated controls 24 h after the initial stimulation, the maximal increase in IL-32 protein expression occurred on day 7 (brown line and points in Fig. 1I).

IL-32 in GBM

Based on the findings in the lung, we hypothesized that expression of IL-32 may be associated with augmented proliferation of ECs. To examine this hypothesis, we stained tissue sections from GBM, which is a malignant brain tumor where EC growth (angiogenesis) is of critical importance for tumor growth. Again, we observed only occasional staining of IL-32 in unaffected areas of the brain. The tumor cells, however, showed massive expression of IL-32 protein (red arrows in Fig. 2). Negative control experiments were performed as described in the previous section and did not exhibit any color changes (data not shown).

siIL-32 reduces the proliferation of ECs, but changes in IL-32 protein abundance do not affect EC apoptosis

Nearly all of the experiments in this study in which siIL-32 was used were performed together with those we have previously published (4). In fact, the same supernatants and lysates were used in most cases; therefore, Fig. 3A and 3B, which show the concentration-dependent knockdown of IL-32 protein by siIL-32 compared with scrambled siRNA without (Fig. 3A) or with IL-1β stimulation (Fig. 3B), are recycled from our earlier studies (4).

Because the abundance of IL-32 was increased in hyperproliferative ECs, we reasoned that silencing of this cytokine should result in a reduction of proliferation of HUVECs. When we knocked down IL-32 with siRNA, we observed that a reduction of IL-32 protein had moderate effects on cell numbers in vehicle-treated HUVECs (left pair of bars in Fig. 3C). However, upon stimulation with IL-1β, a reduction of IL-32 by 76% resulted in a decrease in proliferation from +58% in scrambled siRNA-transfected HUVECs to −15% (right pair of bars in Fig. 3C). To gather additional evidence, we used an MTS assay in which the production of dye is proportional to the number of live cells. As shown in Fig. 3D, the proliferation of IL-1β–stimulated HUVECs was reduced by >50% upon silencing of IL-32 compared with scrambled siRNA-transfected cells. Similar to Fig. 3C, the effect was less pronounced in unstimulated HUVECs.

Next, we performed experiments to answer the important question of whether the reduction in cell numbers conferred by siIL-32 was due to an increase in apoptosis or truly due to a decrease in proliferation. Using flow cytometric quantification of annexin V to detect the presence of ongoing apoptosis and propidium iodide (PI) to identify cells during late apoptosis and necrosis, we found that siIL-32 conferred a moderate (statistically not significant) increase of annexin V and PI in HUVECs (up to 1.4-fold ± 11% more annexin V and up to 1.2-fold ± 9% more PI compared with scrambled siRNA; $n = 6$, $p > 0.2$). In pulmonary microvascular ECs, this trend was slightly more pronounced but still not significant with 1.7-fold ± 0.32% more annexin V and 1.6-fold ± 41% more PI with siIL-32 ($n = 8$, $p > 0.1$). Furthermore, we performed measurements of LDH in the culture supernatants, which also showed that siIL-32 did not result in an increase in cell death (no difference between scrambled and siRNA to IL-32). To be as certain as possible about this crucial

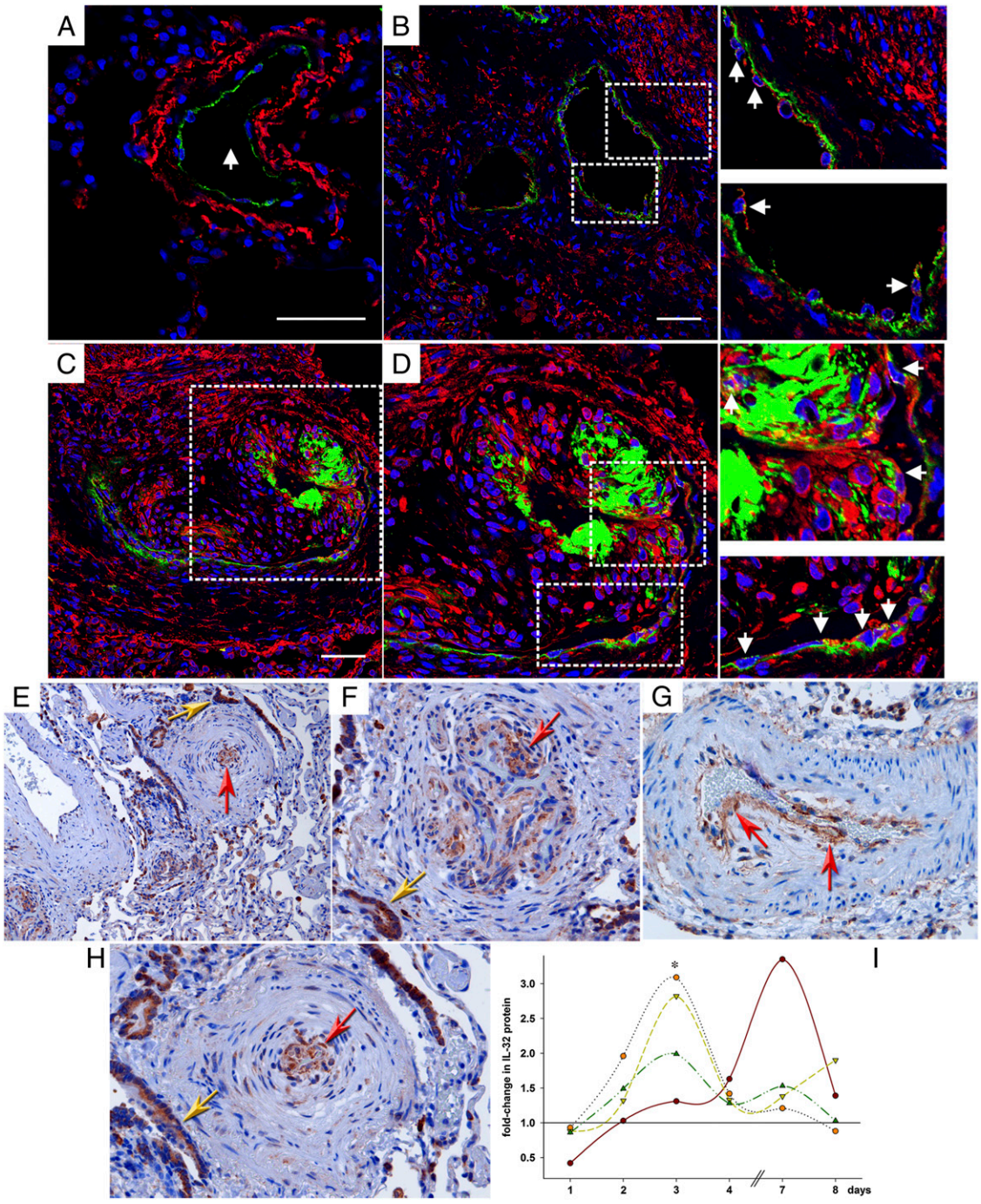

FIGURE 1. IL-32 in PAH. (**A**–**D**) Triple-label immunofluorescence images of human lung vessels. IL-32 is stained in red, vWF in green, and nuclei in blue (DAPI). Scale bar, 50 μm. (A) Staining of a normal pulmonary arteriole (arrow) from a patient not suffering from PAH. Image is representative of three similar results. (B–D) Specimen from one out of a total of three similar patients with idiopathic PAH. (B) An affected but not obliterated arteriole with activated ECs is depicted. Dotted lines indicate areas that are enlarged in insets on *right*. The arrowheads point to EC expression of IL-32. (C, D) A plexiform lesion is shown, in which the lumen of the blood vessel is obliterated by hyperproliferative ECs. Dotted line indicates area that is enlarged in (D), and yet more detail is provided in insets on *right*. The arrowheads point to the hyperproliferative ECs that stain positive for IL-32 and vWF. (**E**–**H**) Classical immunohistochemistry of IL-32 in lung specimen of PAH patients. After incubation with the primary Ab to IL-32, slides were stained with diaminobenzidine and hematoxylin. Diseased, hyperproliferative pulmonary blood vessels with a markedly thickened endothelium are shown in overview in (E) (original magnification ×100) and in detail in (F)–(H) (original magnification ×200). The innermost endothelial layer contains a considerable amount of IL-32 protein (red arrows). Staining is also seen in alveolar epithelial cells (golden arrows). Images are representative of three patients. (**I**) HUVECs were plated and grown for 24 h. Thereafter, the medium was changed to stimulation medium (2% FCS, see *Materials and Methods*) and either semaxanib (10 μM) or vehicle was added. Cells were harvested after the indicated periods of time and lysates were assayed for IL-32 protein and total protein. IL-32 abundance was normalized to total protein, fold increases in normalized IL-32 abundance were calculated (IL-32 in semaxanib-treated cells divided by IL-32 in vehicle-treated cells), and IL-32 abundance in vehicle-treated cells was set at 1. Each line indicates fold change in semaxanib-treated cells over vehicle-treated cells in one time course experiment ($n = 4$). *$p < 0.05$ for semaxanib versus vehicle.

aspect, we next treated HUVECs with exogenous IL-32γ in the presence or absence of IFN-γ pretreatment (described below) and measured the mRNA abundance of *bak1*, *bcl2*, and *bclxl* by real-time PCR. None of the three mediators of apoptosis exhibited

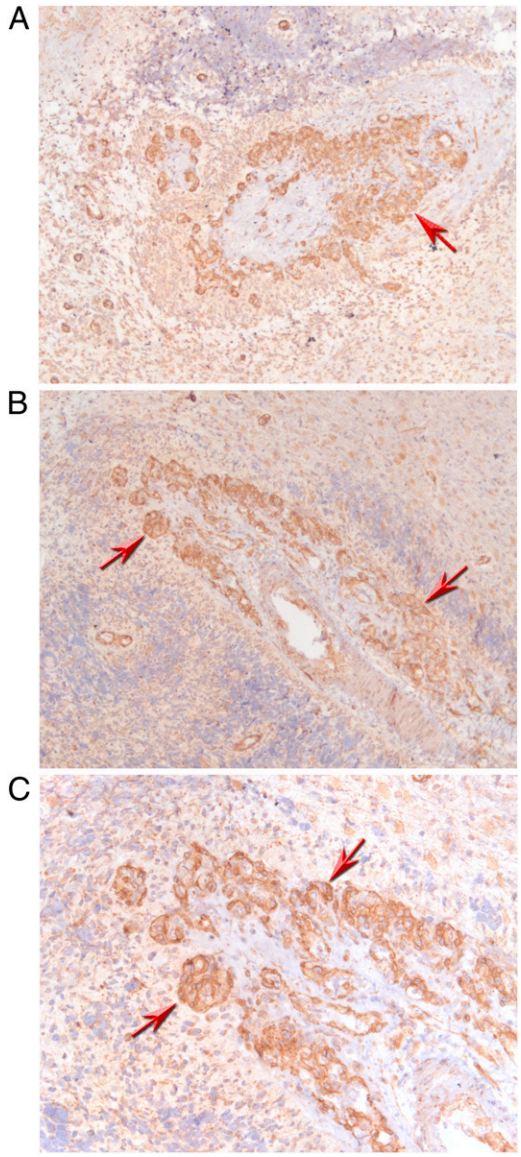

FIGURE 2. IL-32 in GBM. Immunohistochemistry with an Ab against IL-32 in sections of brains affected by GBM was performed and is depicted at an original magnification of ×100 (**A**, **B**) or ×200 (**C**). Strong staining for IL-32 protein is observed in areas affected by the tumor (red arrows). Images are representative for those obtained from a total of three GBM patients.

a significant change in mRNA abundance in IL-32γ–stimulated cells compared with controls (*bak1* up to 19 ± 7% increased, *bcl2* up to 19 ± 6% decreased, and *bclxl* up to 17 ± 7% increased; $n = 4$, $p > 0.3$). These findings are highly unlikely to be an artifact, as the data on IL-8 (which show a pronounced regulation; see Fig. 7G) were obtained from the same samples. Taken together, these data show that the angiogenic effect of IL-32 is not due to a change in apoptotic programming.

siIL-32 in ECs: TGF-β1, NO, and VEGF

We further explored the actions of IL-32 using ECs in which IL-32 was silenced by siRNA and measured the concentrations of TGF-β1 and NO, two mediators known to play a role in PAH (40). As demonstrated in Fig. 3E, we found that the concentration of NO decreased by 61% from 13 to 5 pg/mg total protein in unstimulated HUVECs in which IL-32 was reduced. In contrast, the abundance of TGF-β1 did not change significantly with siIL-32 (data not shown). Unexpectedly, this was the case for VEGF as well; in fact, the abundance of VEGF was slightly though nonsignificantly higher in ECs transfected with siIL-32 (vehicle, 400 ± 72 versus 508 ± 64 pg/mg total protein in scrambled-transfected versus siIL-32–transfected cultures, respectively, $p = 0.09$; IL-1β–stimulated HUVECs, 810 ± 87 versus 1082 ± 195 pg/mg total protein in scr versus siIL-32, $p = 0.54$; $n = 9$).

Pretreatment with IFN-γ sensitizes ECs to exogenous IL-32γ

Next, we attempted to confirm the findings obtained by silencing IL-32 by incubating the HUVECs with exogenous rIL-32γ. We expected to observe inverse effects, but instead exogenous IL-32γ did not affect any of the parameters described previously at concentrations between 1 and 500 ng/ml. However, when HUVECs were pretreated with IFN-γ for 24 h, stimulation with exogenous IL-32γ resulted in the expected findings; in IFN-γ–pretreated cells, the concentrations of IL-32γ needed to elicit IL-6 production were as low as 10 ng/ml. As demonstrated in Fig. 4A, IFN-γ alone conferred a moderate, up to 39%, reduction in the production of IL-6. Treatment with IL-32γ alone had only marginal effects, but together with IFN-γ, the abundance of IL-6 increased up to 2.3-fold over control and 3.8-fold over IFN-γ alone. This increase was dependent on the concentration of both IL-32γ and IFN-γ.

Interestingly, the sensitization effect was specific to IFN-γ. We also pretreated the HUVEC cultures with IL-1β (1 and 10 ng/ml), LPS (10 and 100 ng/ml), muramyl dipeptide (0.2 and 1 μg/ml), thrombin (0.1 and 0.5 U/ml), or VEGF at 1 and 10 ng/ml, none of which increased the responsiveness of the cells to exogenous IL-32γ.

To further characterize this unexpected effect, we tested whether IFN-γ pretreatment increased the response to a different preparation of exogenous IL-32γ in a different cell type. We generated a completely synthetic IL-32γ peptide and added this protein to PBMC cultures that had been pretreated with IFN-γ or vehicle. Fig. 4B and 4C show that IFN-γ indeed sensitized PBMCs. The abundance of IL-6 was up to 8-fold higher and that of TNF was up to 24-fold increased compared with exogenous synthetic IL-32γ alone, whereas the effects of IFN-γ alone were negligible.

In vivo angiogenesis assays (matrigel)

To obtain in vivo evidence for the angiogenic properties of IL-32, we employed the matrigel method (41, 42). Growth factor–reduced matrigel was loaded with two different concentrations of rIL-32γ (25 and 100 ng/ml), VEGF (25 ng/ml) for positive control, or vehicle for negative control and injected s.c. The plugs and the surrounding tissue were harvested 14 d later. After cutting, the sections were stained for the endothelial marker CD31 and then analyzed for the formation of capillaries using both a semiquantitative scoring system, in which 0 represented no change, 4 stood for maximum change, and 1, 2, and 3 for intermediate levels of change, as well as an automated algorithm that was based on $CD31^+$ cells. Functionality of the new vessels was ascertained by confirming the presence of RBCs within them. Additionally, we assessed the infiltration of the plugs by other cells, which were identified by morphology and subjected to the semiquantitative scoring system described above.

Most importantly, we observed that, compared with vehicle, 100 ng/ml IL-32γ in the matrigel plug induced a marked angiogenic response; in fact, this response was stronger than that of 25 ng/ml VEGF. Fig. 5 shows slides representative of this effect. Whereas in the VEGF-loaded plugs (a representative one shown in Fig. 5B) the mean score for the formation of new capillaries was 1.65, that score was 1.70 in the plugs loaded with 100 ng/ml IL-32γ (ex-

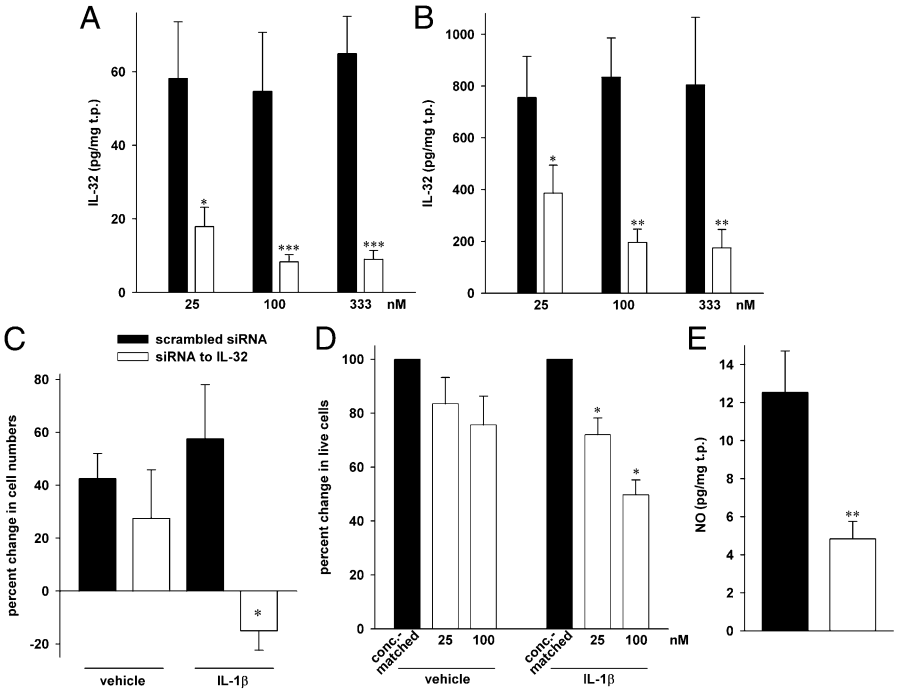

FIGURE 3. Proliferation and NO abundance after silencing of IL-32 in HUVECs. (**A** and **B**) These panels are reprinted with permission from Nold-Petry et al. (4), because the results in this figure were obtained from the same lysates and supernatants as those in figures 4 and 5 in Ref. 4. Transfection of HUVECs with either the indicated concentrations of siIL-32 or scrambled siRNA was followed by stimulation with 10 ng/ml IL-1β (B) or vehicle (A) for 20 h. Means ± SEM of IL-32 abundance in cell lysates normalized to total protein (t.p.) is depicted; $n = 10$. (**C**) HUVECs were gently detached from the plates and viable cells were counted by hand using the trypan blue exclusion method. The number of cells seeded after transfection was set as baseline. Mean percentage change in siIL-32–transfected cells compared with scr-transfected cells ± SEM is shown ($n = 4$). (**D**) After transfection with the indicated concentration of siIL-32 or the same concentration of scrambled siRNA, cells were plated, IL-1β (10 ng/ml) or vehicle was added, and the cultures were incubated for 3 d. Thereafter, MTS assays were performed. The graph shows means of percentage changes ± SEM in the number of live cells, comparing 25 or 100 nM siIL-32 to the appropriate concentration of scrambled siRNA, which is set at 100% ($n = 6$). (**E**) Supernatants from HUVECs transfected with 100 nM siIL-32 or scrambled siRNA were collected after 48 h and assayed for total nitrate/nitrite concentration. Mean concentration of total NO normalized to total protein (t.p.) ± SEM is depicted ($n = 6$). All statistical comparisons are as follows: $*p < 0.05$, $**p < 0.01$, $***p < 0.001$ for siIL-32 versus scrambled siRNA.

emplary plug at ×10 and ×20 magnification; Fig. 5E and 5F, respectively). Furthermore, 25 ng/ml IL-32γ still resulted in a mean score of 0.78 (Fig. 5C, 5D), with the vehicle-loaded plugs scoring 0.20 (Fig. 5A; a quantitative summary is depicted in Fig. 6A). These results obtained by semiquantitative scoring were confirmed by subjecting the same slides to automated counting using the capillary algorithm of the Aperio software. As shown in Fig. 6B, this method produced similar increases, namely 3.5-, 7-, and 6-fold for 25 and 100 ng/ml IL-32γ and VEGF, respectively, over control. Owing to the greater variation of the data, only the neocapillarization induced by 100 ng/ml IL-32γ was statistically significant when the computer-based analysis was used. The mean vessel area of the neocapillaries induced by IL-32γ was moderately larger than in control and VEGF plugs (49 μm^2 in control and VEGF plugs versus 55 and 72 μm^2 in 25 and 100 ng/ml IL-32γ, respectively; Fig. 6C).

To ascertain specificity, we also performed the matrigel assay with plugs loaded with 10 ng/ml LPS. Angiogenesis in these plugs was equal to that in vehicle controls.

With regard to other observations, the overall cellularity within the implants was mainly composed of inflammatory cells, lipid-containing cells, neocapillaries, and fibroblasts. In the tissue adjacent to the matrigel plugs, the scores for the presence of inflammatory cells as well as fibroblasts showed only minor differences. In the implants, however, IL-32γ induced an increase in lipoidosis at both concentrations (Fig. 6D), whereas this effect was mild and not significant with VEGF. As shown in Fig. 6E, a degree of infiltration with inflammatory cells was observed in each of the slides, and there was no difference between the treatment groups. The inflammatory response was mixed, with both polymorphonuclear cells (PMNs) as well as lymphocytes present. Where the inflammation was more advanced, and extended farther into surrounding tissues, PMNs predominated. When the inflammatory response was minimal or mild, a scattering of PMNs and/or lymphocytes/macrophages was apparent within or associated with the subcutis and fibrous connective tissue layer.

The integrin $\alpha_V\beta_3$ colocalizes with IL-32 in PAH and mediates its angiogenic activities

We recently reported the interaction of IL-32γ with the integrin $\alpha_V\beta_3$ (27). Therefore, we investigated whether this interaction occurred in human PAH. Indeed, confocal microscopy experiments demonstrated that IL-32 colocalized with $\alpha_V\beta_3$ in the plexiform lesions of PAH (Fig. 7B–F), but not in the endothelium of normal pulmonary blood vessels (Fig. 7A), in which the expression of $\alpha_V\beta_3$ was low.

To further explore the mechanisms by which IL-32 exerted its angiogenic properties, we first subjected samples from siIL-32 or scrambled-transfected and vehicle- or IL-1β–stimulated HUVECs to angiogenesis profiling analysis. Consistent with the proangiogenic state conferred by IL-32, we found that the antiangiogenic activin A, endostatin, and angiopoietin 2 were increased 3-, 2-, and 2-fold when IL-32 was reduced, whereas the proangiogenic IL-8, u-plasminogen activator, and matrix metalloproteinase (MMP)-9 were up to 55% decreased. On the other hand, there was

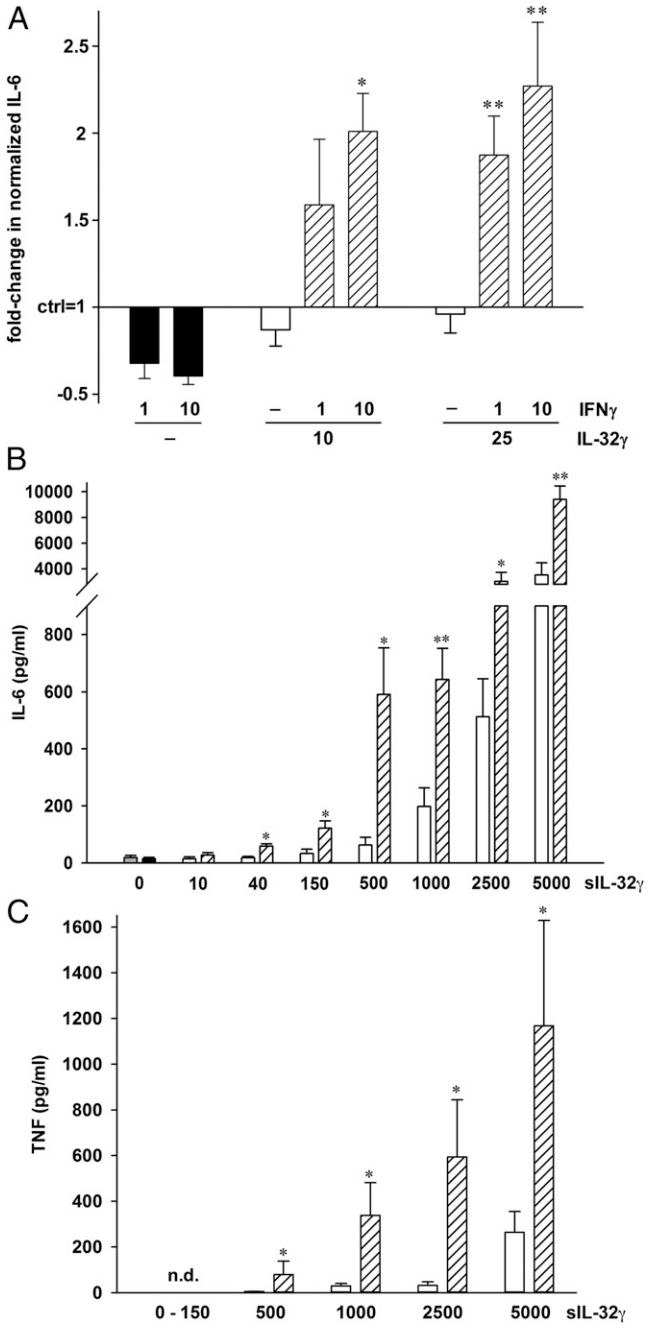

FIGURE 4. IFN-γ sensitizes cells to exogenous IL-32γ. (**A**) After the medium was changed from growth to stimulation medium, HUVECs were treated with the indicated concentrations of IFN-γ (ng/ml) or vehicle for 24 h. Thereafter, rIL-32γ or vehicle was added at the concentrations indicated (ng/ml). IL-6 was measured in the culture supernatants after another 24 h. The graph shows means of fold changes in normalized IL-6 protein abundance comparing vehicle (control, set as 1) with stimulated conditions ± SEM ($n = 7$). *$p < 0.05$, **$p < 0.01$ for IFN-γ alone versus IL-32γ plus IFN-γ. (**B** and **C**) PBMCs were incubated with 10 ng/ml IFN-γ or vehicle for 24 h, followed by addition of synthetic (s)IL-32γ at the indicated final concentrations in ng/ml. Supernatants were harvested 24 h later and assayed for IL-6 (B) and TNF (C). Absolute concentrations of both cytokines ± SEM are depicted ($n = 4$ healthy donors). Gray bar (*far left*), medium alone; black bar (*second from left*), IFN-γ alone; open bars, sIL-32γ alone; striped bars, sIL-32γ plus IFN-γ. *$p < 0.05$, **$p < 0.01$ for sIL-32γ alone versus sIL-32γ plus IFN-γ. n.d., Not detected.

up to 3.5-fold more angiogenin and endoglin in siIL-32–transfected HUVECs under unstimulated conditions, but no change was detected after treatment with IL-1β. Next, we treated HUVEC cultures with exogenous rIL-32γ in the presence or absence of the $\alpha_V\beta_3$ inhibitor cyclo(Arg-Gly-Asp-D-Phe-Val) and of IFN-γ pretreatment and performed real-time PCR analysis. As shown in Fig. 7G, exogenous IL-32γ dose-dependently induced IL-8 but only when the cells were pretreated with IFN-γ (up to 2.5-fold over IFN-γ alone). Importantly, blockade of the integrin $\alpha_V\beta_3$ reduced the IL-32γ plus IFN-γ–induced increase in IL-8 mRNA by up to 85%. We also performed PCR analysis of the other mediators of angiogenesis that exhibited a change on the profiler; these experiments showed a reduction by IL-32γ plus IFN-γ and a blockade of the effect by the $\alpha_V\beta_3$ inhibitor for activin A, but only small changes for the other mediators. This weaker effect of exogenous IL-32 even with IFN-γ pretreatment in comparison with siIL-32 is consistent with our previous experience with this cytokine (9, 16).

To demonstrate that $\alpha_V\beta_3$ indeed contributes to the angiogenic effects of IL-32, we next performed an angiogenesis assay in which HUVECs or human aortic ECs (HAoECs) were cocultured with human dermal fibroblasts (43). In this assay, exogenous rIL-32γ did not require IFN-γ, but without a costimulus markedly increased tube formation in a dose-dependent fashion (up to 3-fold; Fig. 8). Consistent with the regulation of IL-8 described above, the IL-32–induced angiogenesis was dependent on functional $\alpha_V\beta_3$, as cyclo(Arg-Gly-Asp-D-Phe-Val) potently reduced the angiogenetic activity of IL-32γ (by up to 72%; Fig. 8B, 8C). In HAoECs, the angiogenetic activity of IL-32γ at 100 ng/ml was comparable to that of 40 ng/ml VEGF (3-fold versus 3.6-fold increase in tube formation), thus resembling our findings in the matrigel experiments. This effect was somewhat weaker, although still significant, in the HUVECs (2-fold versus 3.5-fold increase in tube formation).

Discussion

The major finding of our investigation is the discovery that IL-32 possesses angiogenic properties. Additionally, we revealed that these properties, which are at least in part mediated by the integrin $\alpha_V\beta_3$, are relevant in vivo (exemplified by examination of ECs in PAH and GBM), and are not mediated by VEGF. Moreover, we demonstrate that pretreatment with IFN-γ sensitizes ECs of neonatal as well as adult pulmonary origin to exogenous IL-32γ, which without IFN-γ is inactive when used as a stimulant in these cells. This finding may be clinically relevant, as there is some evidence that IFN-γ may play a detrimental role in PAH (44, 45). In coculture of HUVECs or HAoECs with HSF and in vivo in matrigel assays, IFN-γ was not required, and exogenous IL-32γ effectively induced angiogenesis when added alone. However, the preparation of recombinant human IL-32γ we used contained a small amount of LPS (see later in the article). This small quantity of LPS, or another factor present in these complex experimental systems, may have substituted for IFN-γ in providing a cofactor that renders IL-32 functional. This concept is backed by similar data obtained with a completely synthetic IL-32γ preparation, which also required a cofactor (IFN-γ) to exert its biological activity. One possible explanation is that IFN-γ may induce expression and/or transport to the cell surface of the yet unknown receptor for IL-32. Because we moreover confirmed the colocalization and functional relationship between IL-32 and the integrin $\alpha_V\beta_3$, and because integrins are known to be IFN-γ–inducible (46, 47), it is possible that $\alpha_V\beta_3$ may act as a receptor for IL-32 on ECs. In more general terms, these data show that a second signal is necessary to render cells responsive to exogenous IL-32.

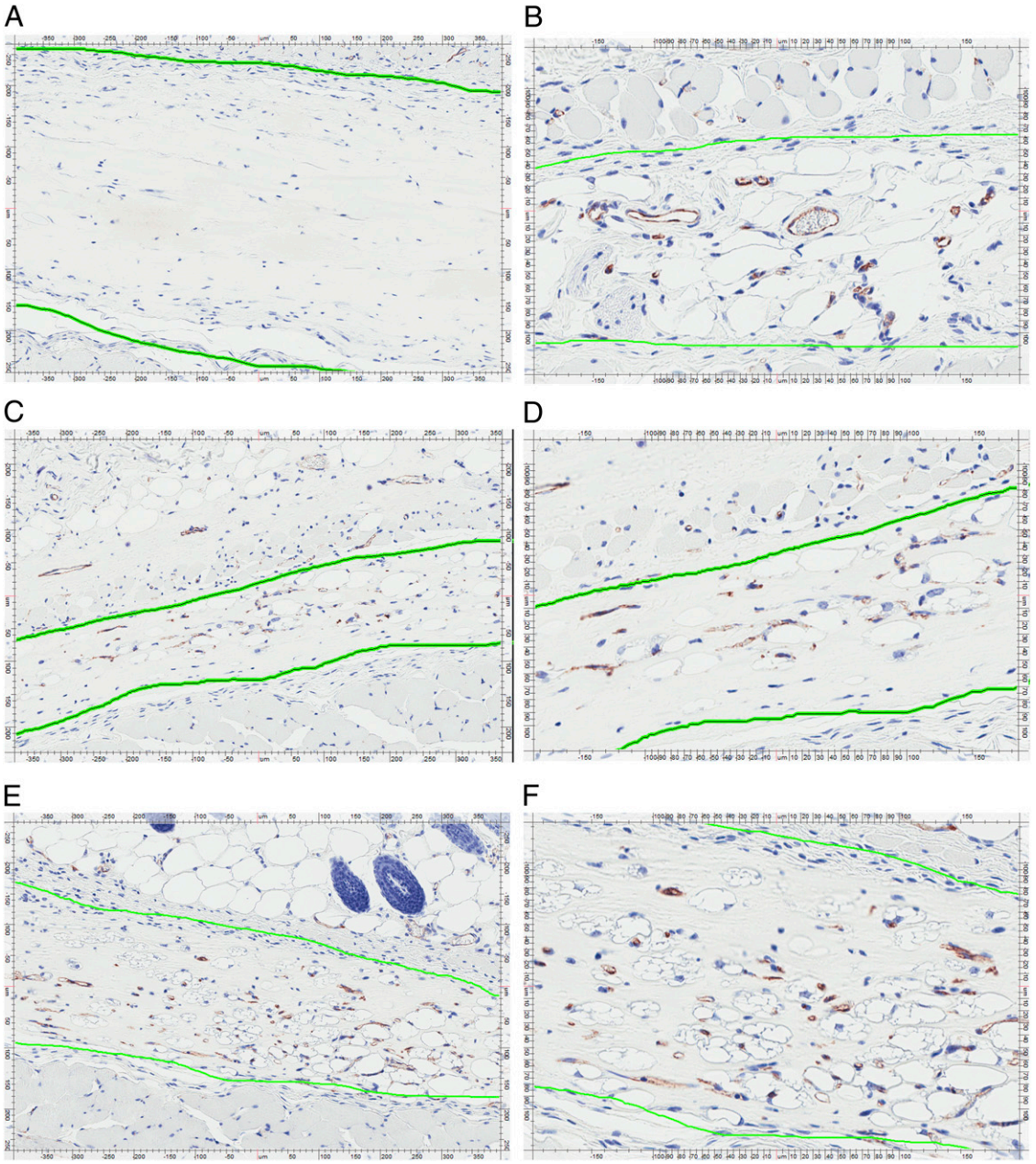

FIGURE 5. IL-32γ induces angiogenesis in vivo. Growth factor–reduced high concentration matrigel was mixed with vehicle (**A**), 25 ng/ml VEGF (**B**), or rIL-32γ at 25 ng/ml (**C**, **D**), or at 100 ng/ml (**E**, **F**); $n = 10$ plugs for each condition. Two 200 μl aliquots of matrigel with nonidentical contents were then injected on the right and left sides of the abdominal wall of male ICR mice. The plugs were harvested 14 d later, followed by cutting and staining for CD31 (chromagens were diaminobenzidine and hematoxylin). The coworkers involved in the analysis of the matrigel experiments were blinded to the reagent with which each individual plug was loaded. Blinding was lifted only after the completion of all aspects of the analysis. Representative plugs loaded with vehicle [(A) original magnification ×10], VEGF at 25 ng/ml [(B) original magnification ×20], or IL-32γ at 25 ng/ml [(C, D) original magnification ×10 and ×20, respectively], or 100 ng/ml [(E, F) original magnification ×10 and ×20, respectively] are depicted. The green line highlights the matrigel plugs, differentiating them from the surrounding tissue, which was left in situ.

We have previously reported that the production of IL-32 protein by ECs is enhanced by various stimuli, most notably by IL-1β, which increases the abundance of IL-32 in EC lysates up to 15-fold, even at low concentrations (4). In that report, we furthermore demonstrated that IL-32 mediates the proinflammatory effects of IL-1β in ECs, as silencing of IL-32 reduced the IL-1β–triggered production of IL-1α, IL-6, IL-8, and ICAM-1 and simultaneously increased the expression of thrombomodulin/CD141.

Each of these proteins has been implicated in the regulation of angiogenesis directly or indirectly, but IL-1 and IL-8 are particularly well established as potent promoters of angiogenesis (for examples, see Refs. 42, 48–51). Therefore, it was a logical next step to explore whether IL-32 itself exerted any effects on the proliferation of EC.

We localized IL-32 to the abnormal ECs that populate the so-called plexiform lesions in the lungs from patients with idiopathic PAH (34). These complex lung vascular abnormalities are characterized by high expression of hypoxia-inducible factor-1α, VEGF, and VEGF receptor 2 genes and proteins, thus presenting an angiogenic signature (35). One pathogenetic concept is that EC injury and apoptosis occur at sites of precapillary arterial bifurcations (28) and that the remaining apoptosis-resistant ECs undergo a pheno-

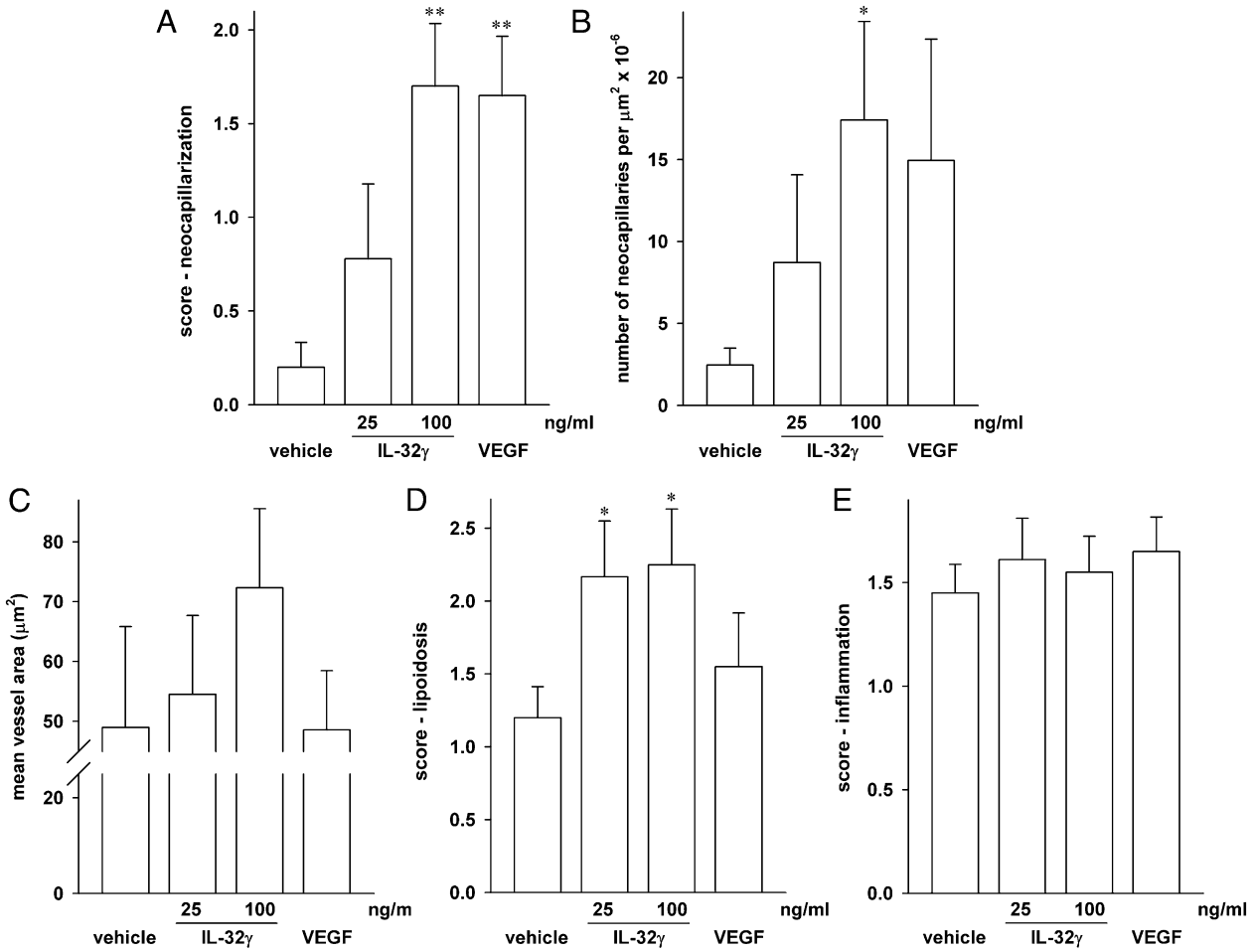

FIGURE 6. Quantitative analysis of neocapillarization, lipoidosis, and influx of inflammatory cells into the matrigel plugs. After cutting and CD31 as well as H&E staining, the slides of the matrigel plugs (n = 10/group) were assessed for the formation of capillaries (**A**, **B**) and for the surface area of these capillaries (**C**), as well as for the presence of adipocytes (**D**) and WBCs (**E**). (A) Neocapillarization was determined by hand-counting and scored semi-quantitatively with 0 representing no increase in neocapillarization, 1 a minimal increase, 2 a mild increase, 3 a moderate increase, and 4 a marked increase in neocapillarization. Mean scores ± SEM are shown. (B) The same slides were assessed by automated analysis using Aperio's microvessel algorithm. The graph depicts means of absolute numbers of microvessels per $\mu m^2 \times 10^{-6}$ ± SEM. (C) Computer-based analysis of the surface area of the capillaries in the plugs. Means of the surface area of the microvessels on each slide ± SEM are shown. (D, E) The same semiquantitative scoring system as in (A) was used to categorize the degree of lipoidosis (D) and inflammation (E). Mean scores ± SEM are shown. *$p < 0.05$ for IL-32γ versus vehicle, **$p < 0.01$ for IL-32γ or VEGF versus vehicle.

typic switch, become hyperproliferative, and eventually obliterate the vascular lumen (31, 35, 52). We have previously characterized this group of angioproliferative lung vascular disorders as quasi-malignant or precancerous (52), but features of immune dysregulation as in autoimmune diseases are also present (53). For example, angioproliferative PAH is associated with the limited form of scleroderma, the so-called CREST syndrome, with systemic lupus erythematosus, and with Sjögren syndrome (30). In this regard, it is interesting that IL-32 appears to regulate the production of NO, which in turn has been implicated in the pathogenesis of PAH (40).

The presence of IL-32 in the angioproliferative plexiform lesions of PAH is also consistent with the expression of this cytokine in psoriatic skin lesions (11, 54), as increased angiogenesis is an important feature of psoriasis. A similar comparison can be made between plexiform lesions and the malignant brain tumor GBM (31), and indeed, we found the abundance of IL-32 protein to be increased in this highly vascularized tumor as well. This is in agreement with another study that screened mRNA levels in this neoplastic disease as well as in breast cancer, where mRNA for IL-32 was also elevated (55).

Together with our previous results, these data suggested that production of IL-32 in ECs was associated with activation and proliferation of these cells. To determine whether IL-32 acts as a causal nexus in the regulation of angioproliferation, we reduced the abundance of this cytokine by siRNA in neonatal HUVECs and adult pulmonary microvascular ECs and HAoECs, and we also employed an in vivo and an in vitro angiogenesis assay. Our finding that reduction of IL-32 arrested the proliferation of HUVECs is consistent with data that IL-1β was found to possess angiogenic properties in matrigel assays (42) and in tumors (56). Similar properties have been described for IL-1α (49, 57), although it should be noted that under different circumstances, IL-1α has been shown to inhibit angiogenesis and tumor growth (58).

Whereas our in vitro proliferation assays showed that IL-32 plays an important role in the proliferation of ECs, both the matrigel studies as well as the coculture experiments demonstrated that an IL-32 gradient did not simply attract ECs in a disorganized fashion. Rather, IL-32 conferred a marked increase in the formation of new EC tubes in the cocultures and new capillaries in the matrigel plugs. The capillaries were functional, as they carried RBCs. In fact, at

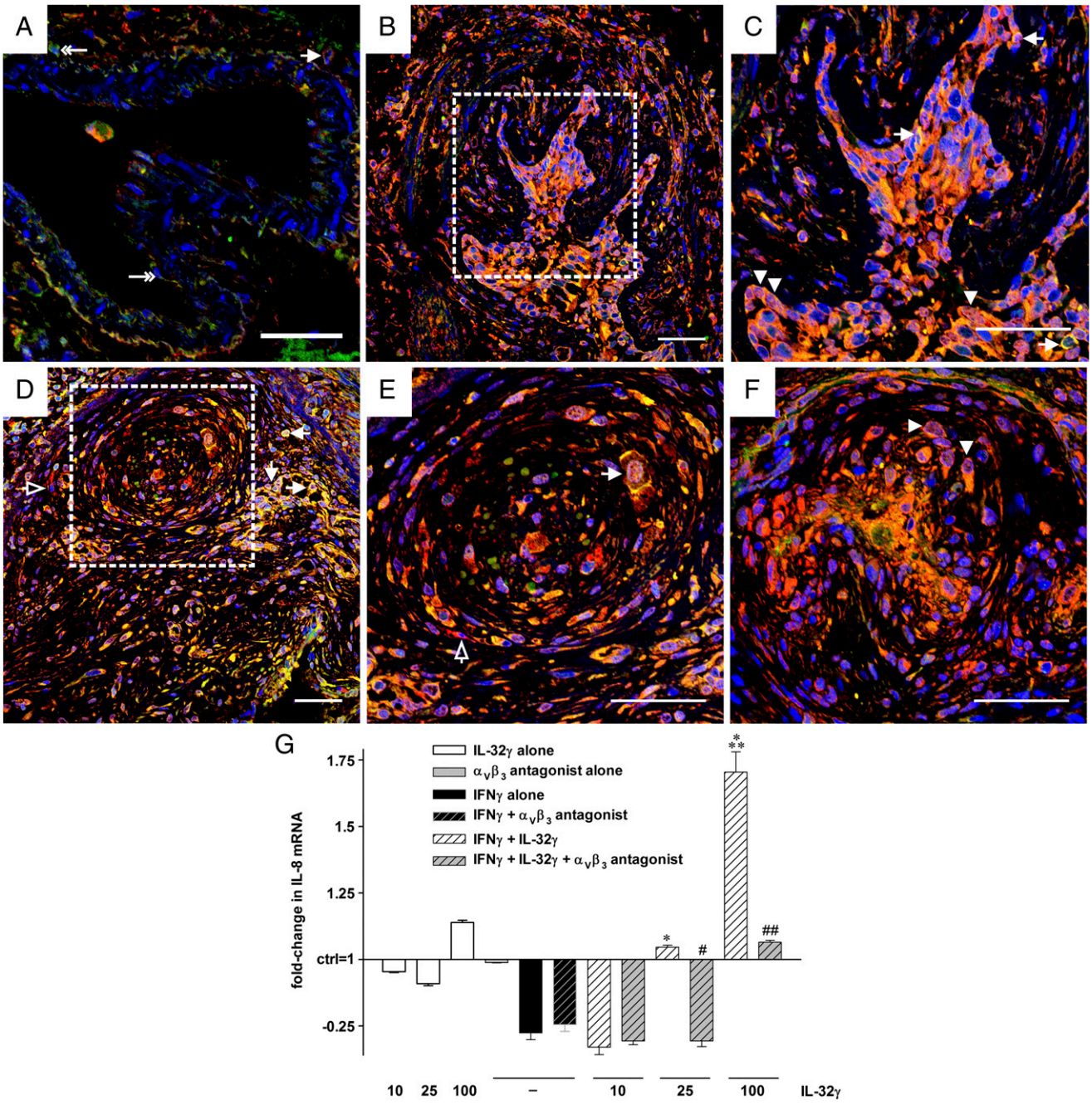

FIGURE 7. Colocalization of integrin $\alpha_V\beta_3$ with IL-32 and functional relevance of the interaction. (**A**–**F**) Representative optical sections acquired by confocal microscopy of double immunofluorescence staining for IL-32 (red) and $\alpha_V\beta_3$ (green). Nuclei are counterstained with DAPI (blue). (A) In lung tissue from a representative control patient (without pulmonary vascular disease) single $\alpha_V\beta_3^+$ cells are seen in the endothelial layer or perivascular region of a pulmonary artery, indicated by double-headed arrow. One $\alpha_V\beta_3^+$/IL-32$^+$ cell (single-headed arrow) was found in the perivascular tissue (cytoplasmic staining). (B–F) In lung tissue from a representative patient, $\alpha_V\beta_3$ colocalized with IL-32 in the plexiform lesions. This colocalization occurred in the nucleus, as indicated by arrowheads, as well as in the cytoplasm and the cell membrane, pointed to by arrows. Cells positive for IL-32 alone are indicated with open arrows. (C) and (E) depict the regions enclosed by the dotted line in (B) and (D), respectively, at higher magnification. Original magnification ×400. Scale bar, 50 μm ($n = 3$ controls and 3 PAH patients). (**G**) HUVECs were pretreated with IFN-γ (10 ng/ml) or vehicle for 24 h, followed by addition of rIL-32γ at the indicated concentrations (ng/ml) and/or the $\alpha_V\beta_3$ inhibitor cyclo(Arg-Gly-Asp-D-Phe-Val) at 10 μM. Six hours thereafter, cells were lysed and subjected to real-time PCR analysis. Fold changes in abundance of IL-8 mRNA normalized to 18S over control (which is set at 1) ± SEM are depicted ($n = 3$). *$p < 0.05$, ***$p < 0.001$ for IFN-γ alone versus IL-32γ plus IFN-γ; $^{\#}p < 0.05$, $^{\#\#}p < 0.01$ for IL-32γ plus IFN-γ versus IL-32γ plus IFN-γ plus cyclo(Arg-Gly-Asp-D-Phe-Val).

100 ng/ml IL-32γ was more efficient at achieving such neocapillarization than 25 ng/ml of the prototypical proangiogenic mediator VEGF. These striking data establish IL-32 as a player on the stages of PAH, neoplastic diseases, and wound healing.

The significance of the larger size of the IL-32–induced new blood vessels compared with those induced by VEGF, as well as the increase in lipoidosis that was also conferred by IL-32γ, will have to be determined. However, the latter observation is intriguing, as one may infer an involvement of IL-32 in atherogenesis; moreover, to our knowledge it represents the first indication for a possible role of this cytokine in obesity. The absence of a difference in the influx of inflammatory cells between IL-32γ and

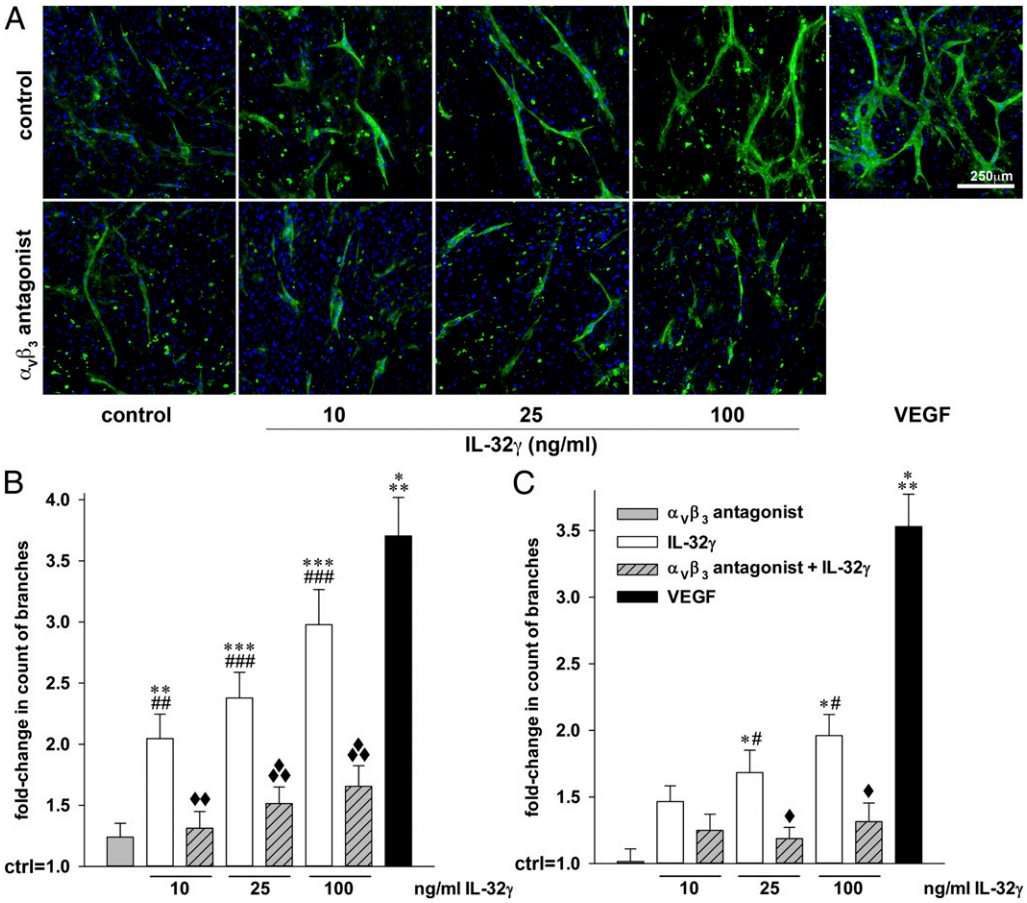

FIGURE 8. IL-32γ–induced in vitro EC tube formation requires functional $\alpha_V\beta_3$. Human dermal fibroblasts were grown to confluence for 3 d, followed by careful addition of HUVECs or HAoECs. Four hours later, treatment with the indicated concentrations of rIL-32γ and/or 10 μM $\alpha_V\beta_3$ inhibitor cyclo (Arg-Gly-Asp-D-Phe-Val) was commenced. Treatment with recombinant human VEGF-165 (40 ng/ml) was used as internal assay control. On day 7 of coculture, newly formed EC tubes were stained with *Sambucus nigra* lectin-FITC (green), nuclei were labeled with DAPI (blue), and the cells were then examined microscopically. Five fields of view per condition were randomly chosen and photographed. (**A**) One represesentative image of five independently performed HAoEC experiments is shown. (**B** and **C**) The number of visible branches in the cocultures containing HAoECs (B) or HUVECs (C) was counted using ImageJ. Graphs illustrate the fold changes in the number of branches of the newly formed EC tubes over vehicle-stimulated cocultures (which are set as 1). $^{*}p < 0.05$, $^{**}p < 0.01$, $^{***}p < 0.001$ for IL-32γ or VEGF versus control. $^{\#}p < 0.05$, $^{\#\#}p < 0.01$, $^{\#\#\#}p < 0.001$ for IL-32γ versus the $\alpha_V\beta_3$ inhibitor. $^{\blacklozenge}p < 0.05$, $^{\blacklozenge\blacklozenge}p < 0.01$, $^{\blacklozenge\blacklozenge\blacklozenge}p < 0.001$ for IL-32γ versus IL-32γ plus the $\alpha_V\beta_3$ inhibitor.

vehicle controls indicates that the angiogenic properties are not dependent on intermediate chemokine release.

It is important to note that the manufacturer tests recombinant human IL-32γ for endotoxin by the *Limulus* amebocyte lysate assay, which does not detect low amounts of LPS. It thus remained unclear whether the reported effects of recombinant human IL-32γ would be identical in the complete absence of microbial products; therefore, we generated a synthetic and completely endotoxin-free IL-32γ in order to eliminate the problems of microbial contamination. The fact that synthetic IL-32γ alone was inactive at 150 and 500 ng/ml supports the pivotal concept that IL-32 requires cofactors such as TLR agonists or IFN-γ for its biological activities. Notwithstanding this fact, because the LPS-loaded matrigel plugs did not differ from those loaded with vehicle, the angiogenic effect was indeed due to IL-32, not the LPS contamination of the recombinant protein preparation.

Importantly, our results not only confirm the recent finding that IL-32 interacts with integrins, but they also demonstrate that the IL-32–induced angiogenesis and cytokine production by ECs are at least in part mediated by the integrin $\alpha_V\beta_3$. We demonstrated interaction of IL-32 with the $\alpha_V\beta_3$ and $\alpha_V\beta_6$ integrins and their downstream signaling intermediates focal adhesion kinase and paxillin (27). Integrins, including $\alpha_V\beta_3$ (59), and focal adhesion kinase (60, 61), contribute to angiogenesis and inhibitors of $\alpha_V\beta_3$ inhibit this process (62); therefore, focal adhesion kinase may also contribute to the proangiogenic properties of IL-32 and $\alpha_V\beta_3$. The high expression of the $\alpha_V\beta_3$ integrin in lung endothelial cells in a rat model of severe PAH has recently been reported (63). Furthermore, our data suggest that IL-32 may use IL-8, u-plasminogen activator, and/or MMP-9 while subduing the antiangiogenic properties of activin A, endostatin, and/or angiopoietin 2 to achieve its proangiogenic programing of ECs.

Of note, although we did observe a mild trend toward an increase in cell death in ECs when there was less IL-32, it should be stated that changes in the abundance of IL-32 did not significantly affect the regulation of apoptosis in these cells; for example, Bak-1, Bcl-2, Bcl-x_L, and lactate dehydrogenase remained unchanged. We infer that at least in ECs, IL-32 has moderate effects on apoptotic programs at best. The effect of this cytokine on cell cycle–related pathways was not part of this study, but it is an interesting topic of further research.

Although not in ECs, the role of IL-32 in apoptosis and cancer has been investigated previously; however, the results of these studies are not homogeneous. On the one hand, IL-32γ over-

expression resulted in reduced growth of melanoma and colon cancer in mice and was associated with reduced expression of antiapoptotic genes such as *bcl2* and *iap* and an increase in *caspase3* and *caspase9* (25). Other studies found that IL-32 contributed to activation-induced cell death in normal T cells (2), HEK cells, HeLa cells, and *Mycobacterium tuberculosis*–stimulated THP-1 cells, and that IL-32γ–induced apoptosis was dependent on caspase-3 (5). In contrast, siIL-32 transfected into bone marrow stromal cells conferred reduced apoptosis in malignant cells in chronic myelomonocytic leukemia (22), and it was also shown to induce the proliferation of hematopoietic progenitor cells (64). In pancreatic cancer, silencing of IL-32 suppressed apoptosis and mRNA expression of *bcl2*, *bclxl*, and *mcl1* (23). Importantly, IL-32 was also demonstrated to be associated with a more malignant and invasive phenotype of lung cancer, and IL-32 levels correlated with those of IL-6, IL-8, and VEGF as well as with a higher microvessel density in the tumors and a poor clinical outcome (24). It appears likely that the overall effect of IL-32 on apoptosis and cancer growth in experimental models depends on the cell type in which this cytokine is (over)expressed or blocked and whether other factors such as immune cells are a part of the respective model.

Only a few studies have investigated IL-32 in the biology of the endothelium—among them our own (4, 16) and some others (55, 64–67)—but these studies mainly focused on the role of IL-32 in endothelial inflammation. In addition to our own finding that VEGF was unaffected by silencing of IL-32 in ECs, others have reported the following data related to VEGF. Treatment of ECs with VEGF did not change the abundance of IL-32 protein (4); blockade of IL-32 by siRNA reduced the production of VEGF from a human bone marrow stroma cell line (22); and the abundance of IL-32 correlated with that of VEGF in lung cancer (24). The last two studies as well as the data we present in this study appear to contrast with the report of an increase in VEGF abundance in human bronchial epithelial cells stimulated with cytokines or rhinovirus after silencing of IL-32 (68). Supernatants from these cells conferred enhanced angiogenesis in HUVECs in vitro. This study was conducted in the setting of asthma, and IL-32 was silenced in epithelial cells, not ECs. Overall, the data obtained in ECs in this study and in those of others favor the conclusion that the angiogenesis driven by IL-32 is not mediated by VEGF.

In conclusion, we further expand the portfolio of properties of IL-32, adding angiogenesis to the functions of this versatile cytokine. Mechanistically, these proangiogenetic activities likely use regulation of IL-8, MMP-9, activin A, and endostatin, but not VEGF or TGF-β1. A second signal is required to render cells responsive to exogenous IL-32, and IL-32-induced angiogenesis is at least in part dependent on the integrin $\alpha_V\beta_3$. Therefore, IL-32 emerges as a key nexus in endothelial cell biology at which the pathways of inflammation and angiogenesis converge.

Acknowledgments

We are grateful for outstanding technical assistance by Nana Burns.

Disclosures

The authors have no financial conflicts of interest.

References

1. Kim, S. H., S. Y. Han, T. Azam, D. Y. Yoon, and C. A. Dinarello. 2005. Interleukin-32: a cytokine and inducer of TNFα. *Immunity* 22: 131–142.
2. Goda, C., T. Kanaji, S. Kanaji, G. Tanaka, K. Arima, S. Ohno, and K. Izuhara. 2006. Involvement of IL-32 in activation-induced cell death in T cells. *Int. Immunol.* 18: 233–240.
3. Imaeda, H., A. Andoh, T. Aomatsu, R. Osaki, S. Bamba, O. Inatomi, T. Shimizu, and Y. Fujiyama. 2011. A new isoform of interleukin-32 suppresses IL-8 mRNA expression in the intestinal epithelial cell line HT-29. *Mol Med Rep* 4: 483–487.
4. Nold-Petry, C. A., M. F. Nold, J. A. Zepp, S. H. Kim, N. F. Voelkel, and C. A. Dinarello. 2009. IL-32-dependent effects of IL-1β on endothelial cell functions. *Proc. Natl. Acad. Sci. USA* 106: 3883–3888.
5. Heinhuis, B., M. G. Netea, W. B. van den Berg, C. A. Dinarello, and L. A. Joosten. 2012. Interleukin-32: a predominantly intracellular proinflammatory mediator that controls cell activation and cell death. *Cytokine* 60: 321–327.
6. Heinhuis, B., M. I. Koenders, F. A. van de Loo, M. G. Netea, W. B. van den Berg, and L. A. Joosten. 2011. Inflammation-dependent secretion and splicing of IL-32γ in rheumatoid arthritis. *Proc. Natl. Acad. Sci. USA* 108: 4962–4967.
7. Novick, D., M. Rubinstein, T. Azam, A. Rabinkov, C. A. Dinarello, and S. H. Kim. 2006. Proteinase 3 is an IL-32 binding protein. *Proc. Natl. Acad. Sci. USA* 103: 3316–3321.
8. Kim, S., S. Lee, E. Her, S. Bae, J. Choi, J. Hong, J. Jaekal, D. Yoon, T. Azam, C. A. Dinarello, and S. Kim. 2008. Proteinase 3-processed form of the recombinant IL-32 separate domain. *BMB Rep* 41: 814–819.
9. Nold, M. F., C. A. Nold-Petry, G. B. Pott, J. A. Zepp, M. T. Saavedra, S. H. Kim, and C. A. Dinarello. 2008. Endogenous IL-32 controls cytokine and HIV-1 production. *J. Immunol.* 181: 557–565.
10. Calabrese, F., S. Baraldo, E. Bazzan, F. Lunardi, F. Rea, P. Maestrelli, G. Turato, K. Lokar-Oliani, A. Papi, R. Zuin, et al. 2008. IL-32, a novel proinflammatory cytokine in chronic obstructive pulmonary disease. *Am. J. Respir. Crit. Care Med.* 178: 894–901.
11. Dinarello, C. A., and S. H. Kim. 2006. IL-32, a novel cytokine with a possible role in disease. *Ann. Rheum. Dis.* 65(Suppl. 3): iii61–iii64.
12. Jeong, H. J., S. Y. Shin, H. A. Oh, M. H. Kim, J. S. Cho, and H. M. Kim. 2011. IL-32 up-regulation is associated with inflammatory cytokine production in allergic rhinitis. *J. Pathol.* 224: 553–563.
13. Na, S. J., S. H. So, K. O. Lee, and Y. C. Choi. 2011. Elevated serum level of interleukin-32α in the patients with myasthenia gravis. *J. Neurol.* 258: 1865–1870.
14. Cagnard, N., F. Letourneur, A. Essabbani, V. Devauchelle, S. Mistou, A. Rapinat, C. Decraene, C. Fournier, and G. Chiocchia. 2005. Interleukin-32, CCL2, PF4F1 and GFD10 are the only cytokine/chemokine genes differentially expressed by in vitro cultured rheumatoid and osteoarthritis fibroblast-like synoviocytes. *Eur. Cytokine Netw.* 16: 289–292.
15. Joosten, L. A., M. G. Netea, S. H. Kim, D. Y. Yoon, B. Oppers-Walgreen, T. R. Radstake, P. Barrera, F. A. van de Loo, C. A. Dinarello, and W. B. van den Berg. 2006. IL-32, a proinflammatory cytokine in rheumatoid arthritis. *Proc. Natl. Acad. Sci. USA* 103: 3298–3303.
16. Zepp, J. A., C. A. Nold-Petry, C. A. Dinarello, and M. F. Nold. 2011. Protection from RNA and DNA viruses by IL-32. *J. Immunol.* 186: 4110–4118.
17. Li, W., W. Sun, L. Liu, F. Yang, Y. Li, Y. Chen, J. Fang, W. Zhang, J. Wu, and Y. Zhu. 2010. IL-32: a host proinflammatory factor against influenza viral replication is upregulated by aberrant epigenetic modifications during influenza A virus infection. *J. Immunol.* 185: 5056–5065.
18. Pan, X., H. Cao, J. Lu, X. Shu, X. Xiong, X. Hong, Q. Xu, H. Zhu, G. Li, and G. Shen. 2011. Interleukin-32 expression induced by hepatitis B virus protein X is mediated through activation of NF-κB. *Mol. Immunol.* 48: 1573–1577.
19. Moschen, A. R., T. Fritz, A. D. Clouston, I. Rebhan, O. Bauhofer, H. D. Barrie, E. E. Powell, S. H. Kim, C. A. Dinarello, R. Bartenschlager, et al. 2011. Interleukin-32: a new proinflammatory cytokine involved in hepatitis C virus-related liver inflammation and fibrosis. *Hepatology* 53: 1819–1829.
20. Lee, S., J. H. Kim, H. Kim, J. W. Kang, S. H. Kim, Y. Yang, J. Kim, J. Park, S. Park, J. Hong, and D. Y. Yoon. 2011. Activation of the interleukin-32 pro-inflammatory pathway in response to human papillomavirus infection and over-expression of interleukin-32 controls the expression of the human papillomavirus oncogene. *Immunology* 132: 410–420.
21. Nishimoto, K. P., A. K. Laust, and E. L. Nelson. 2008. A human dendritic cell subset receptive to the Venezuelan equine encephalitis virus-derived replicon particle constitutively expresses IL-32. *J. Immunol.* 181: 4010–4018.
22. Marcondes, A. M., A. J. Mhyre, D. L. Stirewalt, S. H. Kim, C. A. Dinarello, and H. J. Deeg. 2008. Dysregulation of IL-32 in myelodysplastic syndrome and chronic myelomonocytic leukemia modulates apoptosis and impairs NK function. *Proc. Natl. Acad. Sci. USA* 105: 2865–2870.
23. Nishida, A., A. Andoh, O. Inatomi, and Y. Fujiyama. 2009. Interleukin-32 expression in the pancreas. *J. Biol. Chem.* 284: 17868–17876.
24. Sorrentino, C., and E. Di Carlo. 2009. Expression of IL-32 in human lung cancer is related to the histotype and metastatic phenotype. *Am. J. Respir. Crit. Care Med.* 180: 769–779.
25. Oh, J. H., M. C. Cho, J. H. Kim, S. Y. Lee, H. J. Kim, E. S. Park, J. O. Ban, J. W. Kang, D. H. Lee, J. H. Shim, et al. 2011. IL-32γ inhibits cancer cell growth through inactivation of NF-κB and STAT3 signals. *Oncogene* 30: 3345–3359.
26. Ciccia, F., R. Alessandro, A. Rizzo, S. Principe, F. Raiata, A. Cavazza, G. Guggino, A. Accardo-Palumbo, L. Boiardi, A. Ferrante, et al. 2011. Expression of IL-32 in the inflamed arteries of patients with giant cell arteritis. *Arthritis Rheum.* 63: 2097–2104.
27. Heinhuis, B., M. I. Koenders, W. B. van den Berg, M. G. Netea, C. A. Dinarello, and L. A. Joosten. 2012. Interleukin 32 (IL-32) contains a typical α-helix bundle structure that resembles focal adhesion targeting region of focal adhesion kinase-1. *J. Biol. Chem.* 287: 5733–5743.
28. Cool, C. D., J. S. Stewart, P. Werahera, G. J. Miller, R. L. Williams, N. F. Voelkel, and R. M. Tuder. 1999. Three-dimensional reconstruction of pulmonary arteries in plexiform pulmonary hypertension using cell-specific markers. Evidence for a dynamic and heterogeneous process of pulmonary endothelial cell growth. *Am. J. Pathol.* 155: 411–419.

29. Hassoun, P. M., L. Mouthon, J. A. Barberà, S. Eddahibi, S. C. Flores, F. Grimminger, P. L. Jones, M. L. Maitland, E. D. Michelakis, N. W. Morrell, et al. 2009. Inflammation, growth factors, and pulmonary vascular remodeling. *J. Am. Coll. Cardiol.* 54(1, Suppl.): S10–S19.
30. Nicolls, M. R., L. Taraseviciene-Stewart, P. R. Rai, D. B. Badesch, and N. F. Voelkel. 2005. Autoimmunity and pulmonary hypertension: a perspective. *Eur. Respir. J.* 26: 1110–1118.
31. Tuder, R. M., B. Groves, D. B. Badesch, and N. F. Voelkel. 1994. Exuberant endothelial cell growth and elements of inflammation are present in plexiform lesions of pulmonary hypertension. *Am. J. Pathol.* 144: 275–285.
32. Humbert, M., G. Monti, F. Brenot, O. Sitbon, A. Portier, L. Grangeot-Keros, P. Duroux, P. Galanaud, G. Simonneau, and D. Emilie. 1995. Increased interleukin-1 and interleukin-6 serum concentrations in severe primary pulmonary hypertension. *Am. J. Respir. Crit. Care Med.* 151: 1628–1631.
33. Tuder, R. M., and N. F. Voelkel. 1998. Pulmonary hypertension and inflammation. *J. Lab. Clin. Med.* 132: 16–24.
34. Voelkel, N. F., J. G. Gomez-Arroyo, A. Abbate, H. J. Bogaard, and M. R. Nicolls. 2012. Pathobiology of pulmonary arterial hypertension and right ventricular failure. *Eur. Respir. J.* 40: 1555–1565.
35. Tuder, R. M., M. Chacon, L. Alger, J. Wang, L. Taraseviciene-Stewart, Y. Kasahara, C. D. Cool, A. E. Bishop, M. Geraci, G. L. Semenza, et al. 2001. Expression of angiogenesis-related molecules in plexiform lesions in severe pulmonary hypertension: evidence for a process of disordered angiogenesis. *J. Pathol.* 195: 367–374.
36. Canavese, M., F. Altruda, T. Ruzicka, and J. Schauber. 2010. Vascular endothelial growth factor (VEGF) in the pathogenesis of psoriasis: a possible target for novel therapies? *J. Dermatol. Sci.* 58: 171–176.
37. Hackeng, T. M., J. A. Fernández, P. E. Dawson, S. B. Kent, and J. H. Griffin. 2000. Chemical synthesis and spontaneous folding of a multidomain protein: anticoagulant microprotein S. *Proc. Natl. Acad. Sci. USA* 97: 14074–14078.
38. Nold, M. F., C. A. Nold-Petry, J. A. Zepp, B. E. Palmer, P. Bufler, and C. A. Dinarello. 2010. IL-37 is a fundamental inhibitor of innate immunity. *Nat. Immunol.* 11: 1014–1022.
39. Sakao, S., L. Taraseviciene-Stewart, J. D. Lee, K. Wood, C. D. Cool, and N. F. Voelkel. 2005. Initial apoptosis is followed by increased proliferation of apoptosis-resistant endothelial cells. *FASEB J.* 19: 1178–1180.
40. Humbert, M., N. W. Morrell, S. L. Archer, K. R. Stenmark, M. R. MacLean, I. M. Lang, B. W. Christman, E. K. Weir, O. Eickelberg, N. F. Voelkel, and M. Rabinovitch. 2004. Cellular and molecular pathobiology of pulmonary arterial hypertension. *J. Am. Coll. Cardiol.* 43(12, Suppl. S): 13S–24S.
41. Voronov, E., D. S. Shouval, Y. Krelin, E. Cagnano, D. Benharroch, Y. Iwakura, C. A. Dinarello, and R. N. Apte. 2003. IL-1 is required for tumor invasiveness and angiogenesis. *Proc. Natl. Acad. Sci. USA* 100: 2645–2650.
42. Carmi, Y., E. Voronov, S. Dotan, N. Lahat, M. A. Rahat, M. Fogel, M. Huszar, M. R. White, C. A. Dinarello, and R. N. Apte. 2009. The role of macrophage-derived IL-1 in induction and maintenance of angiogenesis. *J. Immunol.* 183: 4705–4714.
43. Baumer, Y., B. Scholz, S. Ivanov, and B. Schlosshauer. 2011. Telomerase-based immortalization modifies the angiogenic/inflammatory responses of human coronary artery endothelial cells. *Exp. Biol. Med. (Maywood)* 236: 692–700.
44. Wang, W., Y. L. Wang, X. Y. Chen, Y. T. Li, W. Hao, Y. P. Jin, and B. Han. 2011. Dexamethasone attenuates development of monocrotaline-induced pulmonary arterial hypertension. *Mol. Biol. Rep.* 38: 3277–3284.
45. Wort, S. J., M. Ito, P. C. Chou, S. K. Mc Master, R. Badiger, E. Jazrawi, P. de Souza, T. W. Evans, J. A. Mitchell, L. Pinhu, et al. 2009. Synergistic induction of endothelin-1 by tumor necrosis factor alpha and interferon γ is due to enhanced NF-kappaB binding and histone acetylation at specific κB sites. *J. Biol. Chem.* 284: 24297–24305.
46. Lee, M. S., and N. Sarvetnick. 1994. Induction of vascular addressins and adhesion molecules in the pancreas of IFN-γ transgenic mice. *J. Immunol.* 152: 4597–4603.
47. Westphal, J. R., H. W. Willems, W. J. Tax, R. A. Koene, D. J. Ruiter, and R. M. de Waal. 1993. The proliferative response of human T cells to allogeneic IFN-γ-treated endothelial cells is mediated via both CD2/LFA-3 and LFA-1/ICAM-1 and -2 adhesion pathways. *Transpl. Immunol.* 1: 183–191.
48. Farkas, L., J. Gauldie, N. F. Voelkel, and M. Kolb. 2011. Pulmonary hypertension and idiopathic pulmonary fibrosis: a tale of angiogenesis, apoptosis and growth factors. *Am. J. Respir. Cell Mol. Biol.* 45: 1–15.
49. Matsuo, Y., H. Sawai, N. Ochi, A. Yasuda, H. Takahashi, H. Funahashi, H. Takeyama, and S. Guha. 2009. Interleukin-1alpha secreted by pancreatic cancer cells promotes angiogenesis and its therapeutic implications. *J. Surg. Res.* 153: 274–281.
50. Shi, C. S., G. Y. Shi, Y. S. Chang, H. S. Han, C. H. Kuo, C. Liu, H. C. Huang, Y. J. Chang, P. S. Chen, and H. L. Wu. 2005. Evidence of human thrombomodulin domain as a novel angiogenic factor. *Circulation* 111: 1627–1636.
51. Waugh, D. J., and C. Wilson. 2008. The interleukin-8 pathway in cancer. *Clin. Cancer Res.* 14: 6735–6741.
52. Rai, P. R., C. D. Cool, J. A. King, T. Stevens, N. Burns, R. A. Winn, M. Kasper, and N. F. Voelkel. 2008. The cancer paradigm of severe pulmonary arterial hypertension. *Am. J. Respir. Crit. Care Med.* 178: 558–564.
53. Soon, E., A. M. Holmes, C. M. Treacy, N. J. Doughty, L. Southgate, R. D. Machado, R. C. Trembath, S. Jennings, L. Barker, P. Nicklin, et al. 2010. Elevated levels of inflammatory cytokines predict survival in idiopathic and familial pulmonary arterial hypertension. *Circulation* 122: 920–927.
54. Kempuraj, D., P. Conti, M. Vasiadi, K. D. Alysandratos, M. Tagen, D. Kalogeromitros, T. Kourelis, S. Gregoriou, M. Makris, N. G. Stavrianeas, and T. C. Theoharides. 2010. IL-32 is increased along with tryptase in lesional psoriatic skin and is up-regulated by substance P in human mast cells. *Eur. J. Dermatol.* 20: 865–867.
55. Kobayashi, H., and P. C. Lin. 2009. Molecular characterization of IL-32 in human endothelial cells. *Cytokine* 46: 351–358.
56. Shchors, K., E. Shchors, F. Rostker, E. R. Lawlor, L. Brown-Swigart, and G. I. Evan. 2006. The Myc-dependent angiogenic switch in tumors is mediated by interleukin 1beta. *Genes Dev.* 20: 2527–2538.
57. Salven, P., K. Hattori, B. Heissig, and S. Rafii. 2002. Interleukin-1α promotes angiogenesis in vivo via VEGFR-2 pathway by inducing inflammatory cell VEGF synthesis and secretion. *FASEB J.* 16: 1471–1473.
58. Nazarenko, I., R. Marhaba, E. Reich, E. Voronov, M. Vitacolonna, D. Hildebrand, E. Elter, M. Rajasagi, R. N. Apte, and M. Zöller. 2008. Tumorigenicity of IL-1α- and IL-1β-deficient fibrosarcoma cells. *Neoplasia* 10: 549–562.
59. Rüegg, C., O. Dormond, and A. Foletti. 2002. Suppression of tumor angiogenesis through the inhibition of integrin function and signaling in endothelial cells: which side to target? *Endothelium* 9: 151–160.
60. Cabrita, M. A., L. M. Jones, J. L. Quizi, L. A. Sabourin, B. C. McKay, and C. L. Addison. 2011. Focal adhesion kinase inhibitors are potent anti-angiogenic agents. *Mol. Oncol.* 5: 517–526.
61. Shen, T. L., A. Y. Park, A. Alcaraz, X. Peng, I. Jang, P. Koni, R. A. Flavell, H. Gu, and J. L. Guan. 2005. Conditional knockout of focal adhesion kinase in endothelial cells reveals its role in angiogenesis and vascular development in late embryogenesis. *J. Cell Biol.* 169: 941–952.
62. Nisato, R. E., J. C. Tille, A. Jonczyk, S. L. Goodman, and M. S. Pepper. 2003. $\alpha_v\beta_3$ and $\alpha_v\beta_5$ integrin antagonists inhibit angiogenesis in vitro. *Angiogenesis* 6: 105–119.
63. Al Husseini, A., G. Bagnato, L. Farkas, J. Gomez-Arroyo, D. Farkas, S. Mizuno, D. Kraskauskas, A. Abbate, D. B. Van Tassel Pharm, N. F. Voelkel, and H. J. Bogaard. 2012. Thyroid hormone is highly permissive in angioproliferative pulmonary hypertension in rats. *Eur. Respir. J.* 41: 104–114.
64. Moldenhauer, A., M. Futschik, H. Lu, M. Helmig, P. Götze, G. Bal, M. Zenke, W. Han, and A. Salama. 2011. Interleukin 32 promotes hematopoietic progenitor expansion and attenuates bone marrow cytotoxicity. *Eur. J. Immunol.* 41: 1774–1786.
65. Kobayashi, H., J. Huang, F. Ye, Y. Shyr, T. S. Blackwell, and P. C. Lin. 2010. Interleukin-32β propagates vascular inflammation and exacerbates sepsis in a mouse model. *PLoS ONE* 5: e9458.
66. Kobayashi, H., E. M. Yazlovitskaya, and P. C. Lin. 2009. Interleukin-32 positively regulates radiation-induced vascular inflammation. *Int. J. Radiat. Oncol. Biol. Phys.* 74: 1573–1579.
67. Cho, K. A., Y. H. Jun, J. W. Suh, J. S. Kang, H. J. Choi, and S. Y. Woo. 2010. Orientia tsutsugamushi induced endothelial cell activation via the NOD1-IL-32 pathway. *Microb. Pathog.* 49: 95–104.
68. Meyer, N., J. Christoph, H. Makrinioti, P. Indermitte, C. Rhyner, M. Soyka, T. Eiwegger, M. Chalubinski, K. Wanke, H. Fujita, et al. 2012. Inhibition of angiogenesis by IL-32: possible role in asthma. *J. Allergy Clin. Immunol.* 129: 964-973.e7.